A 3D Magnetic Force Manipulator DC Prototype

Leandra Vicci
Microelectronic Systems Laboratory
Department of Computer Science
University of North Carolina at Chapel Hill
17 October 2001
(Rev 2) 4 September 2003

Summary

A potentially useful instrument for the biological sciences would be a 3 dimensional force microscope (3DFM) for measurement of 3 dimensional viscous and elastic fields at sub micrometer scale in-vitro and in-vivo. Substantial development has been conducted on various aspects of this problem, but a general instrument having this capability does not yet exist. All approaches I know of utilize a microscopic bead as a mechanical probe, the position of which can be sensed, and the force on which can be controlled. One force technique is "optical tweezers." This technique requires high optical field intensities which interact strongly with many materials and may produce undesired side effects on in-vivo experiments. Alternatively, magnetic techniques use a magnetic bead driven by low frequency magnetic fields which only interact weakly with most biological materials. Related prior work includes high gradient techniques [Haber00], a close proximity single pole rheometer [Bausch98,99], and a two dimensional manipulator [Amblard96]. To my knowledge, our work is the first attempt to implement a full three dimensional magnetic manipulator. A low frequency (DC) prototype magnetic circuit and drive electronics have been designed and built to explore the capabilities of the magnetic technique for a 3DFM. This report comprises a brief description of the DC prototype, and a complete set of its design documents. This is a report of work in progress, and does not present any results of experiments performed on the prototype.

1 Conceptual design

The magnetic manipulator is intended to be a subsystem to work in concert with other components of a 3DFM. The target was to produce three dimensional nanonewton forces on sub micrometer magnetic beads with a bandwidth of the order of 10^4 [Hz].

A conceptual design phase preceded the design of the first prototype. The conceptual phase began at a very high level of abstraction, leaving many important implementation issues to be determined. This section describes the conceptual design at this abstraction level.

1.1 Spatial coexistence

Whatever magnetic structure is devised, it must provide adequate space to accommodate other subsystems requiring access to the sample under test (SUT).

This includes a sample holder attached to a 3-axis mechanical actuator. Particular attention is paid to the region very local to the SUT in which a liquid sample cell having optical quality cover glasses must be fit. The mounting of the sample cell to actuators and the actuators themselves can occur a small distance away from the SUT where there is less spatial congestion.

It also includes an optical tracking subsystem, the current embodiment of which uses reentrant high numerical aperture (NA) optics which require an unobstructed space comprising two reentrant cones corresponding to the NA of the system. Therefore, under the assumption that the magnetic field geometry is to be formed by using high permeability magnetic cores which are optically opaque, it is desirable that the number of field producing poles be small, and the angular separation between the poles be large. Ostensibly, the minimum number of poles needed to provide forces in three dimensions is four.

1.2 Ideal magnetic circuit

The conceptual design starts with idealized assumptions: a linear, low hysteresis magnetic core material of very high permeability. In this idealization, a magnetic structure can be envisioned with poles converging from a magnetically interconnecting shell to sharpened tips near the SUT, each pole being magnetically driven by a current carrying coil. This situation is reasonably well modeled by a monopole at the location of each tip with strength proportional to the flux induced in its pole by the various coils in the system. The sum of the aggregate monopole strengths in this model must be zero because the coils can only generate dipole magnetization.

1.3 The force equation

The force on a permeable soft magnetic bead is caused by the interaction between an incident magnetic field $\boldsymbol{B}$ and the magnetic dipole moment $\boldsymbol{m}$ induced in the bead by $\boldsymbol{B}$ (see Appendix A). Subject to saturation properties of the bead material,

$$\boldsymbol{m} = \frac{\pi d^3}{2\mu_0}\left(\frac{\mu_r - 1}{\mu_r + 2}\right)\boldsymbol{B}, \qquad \text{[SI units]}$$

where μ_0 is the permeability of free space, μ_r is the relative permeability of the bead, and d is the diameter of the bead. This agrees with the approximate result $\boldsymbol{m} = (4\pi a^3/3\mu_0)\chi \boldsymbol{B}$ published by [Amblard96] in the limit of small $\chi = \mu_r - 1$, where a is the radius of the bead. The force exerted on $\boldsymbol{m}$ by $\boldsymbol{B}$ is,

$$\boldsymbol{F} = \frac{\pi d^3}{2\mu_0}\left(\frac{\mu_r - 1}{\mu_r + 2}\right)\nabla B^2.$$

The magnitude B of the field generated by a magnetic monopole is of the form B_p/r^2 where B_p is the pole strength and r is the distance from the monopole. The corresponding gradient ∇B of the field is $2B_p/r^3$, directed towards the monopole. Thus the force on a bead is towards the monopole, varying as B_p^2/r^5. Clearly, the distance of the monopoles from the bead are of primary concern in the optimizing the magnitude of the force.

1.4 A tetrahedral geometry

A physical approximation of the monopole model uses tapered, high permeability pole cores, radially disposed about the bead location, driven by current carrying coils, with their outer ends connected by a high permeability shell to provide a magnetic flux return path for each core through the other cores. Ideally then, the i^{th} of n physical poles approximates n monopoles, the i^{th} having strength B_i and the others having strengths B_j such that $\sum_{j\neq i}^{n} B_j = -B_i$.

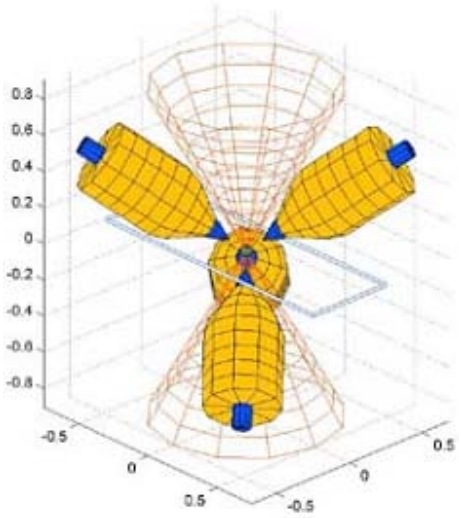

The conceptual design, shown without the outer magnetic return path shell

Since the cores are optically opaque and occupy space, they compete with the system optics for solid angle and with the SUT mechanicals for volume. It is therefore desirable to minimize the number of poles used. Since a monopole force is central, i.e., directed toward the monopole, it takes at least four monopoles to create forces in three dimensions. A symmetric design as shown here comprises four poles converging from the vertices of a virtual equilateral tetrahedron (ET) towards its center. This geometry is fortuitous in that there are three orthogonal lines passing through the center, each having the maximum possible angular separation from the closest poles. This conveniently provides an optical axis normal to a plane for the slide holding the SUT.

Parametric studies showed this geometry to be close to optimal for given pole strength B_0, and separation r_0. Consider k poles of strength B_0/k equally spaced around a circle of radius a, coaxial with $\boldsymbol{r}_0$ at location r_p. The tetrahedron is represented by $n = 3$, $a = 0.94r_0$, $r_p = -0.33r_0$. The force was found to be independent of k for $k > 1$, and within 11% of the maximum, which occurs at $r_p = -0.6$ (see Appendix B).

2 Physical implementation

The conceptual design was done at a very high level of abstraction. This luxury is forfeited in the process of implementing a buildable design. Consequently, a number of trade offs and compromises must be made. The primary goal was to maximize the amount of force attainable without interference to the 0.7 NA optics used by the existing experimental setup.

2.1 Spatial considerations

It was decided not to intrude into the solid angle of the optical path, which comprises two reentrant cones, each with included angle of about 89° . It was also decided not to cut into the lens bodies to accommodate the magnetic poles. The lenses were Mitutoyo M Plan Apochromatic APO100 with a working distance of 6 [mm]. The lens bodies fill an angle of 110° which is very close to the 109.5° included angle between vertices of an ET.

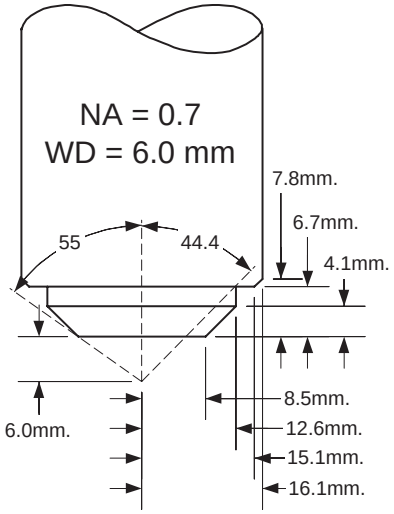

The system lenses

The finite thickness of the magnet poles themselves precludes even approximating the pole angles of the abstract design unless the lens body or the poles are modified with relief cuts. It made more sense to modify pole angles from 35.3° to 22.5° inclination from horizontal, while still placing the pole tips at the vertices of an ET. A pole tip taper angle of 9.5° leaves 7.75° angular clearance from the lens body, but placement of the pole tips on an ET large enough to accommodate the SUT cell uses up nearly all of the linear pole to lens body clearance. (See Appendix C, sheet 1.)

Due to the $1/r^5$ force dependence, the size of the SUT cell is a very strong determiner of the achievable bead force. It was desired that the cells comprise readily available materials, that they provide a reasonably well sealed liquid SUT environment, and that they have adequate optical properties. These factors led to the choice of a sandwich comprising two microscope cover slips separated by Scotch #136 tape (3mil transparent double-backed) with a hole punched to contain the SUT. The thickness of the cell is approximately 440 [μm].

The pole tips are of course not sharp points, but may be regarded as spherical. For very high permeability, the virtual monopole location is approximately at the center of the sphere. Thus for a horizontal cell, the vertical separation between upper and lower monopoles must be at least the sum of the sphere radii (each specified as ≤ 50 [μm]) and the cell thickness. Allowing 160 [μm] clearance for handling and insertion of the cell, the vertical separation of each tip from the center of the cell is 300 [μm], or 350 [μm] vertically from each monopole to the center. The total distance of each monopole from the cell center is $350/\cos(109.5/2) = 606$ [μm]. This is the closest we can reasonably expect to get the monopoles with this SUT cell and design approach.

2.2 Core materials

Second only to compactness, the B^2 force dependence motivated us to maximize the field strength. Even with very high permeability μ_r, leakage flux between poles everywhere except at the tips is wasted flux, and cannot be avoided. Since B is proportional to the magnetomotive force (MMF), or Ampere turns linking the magnetic path, this can be compensated at the expense of coil size and current. Of course there are thermal limitations due to resistive losses in the coils.

For high μ_r the B field is also strongly dependent on the geometry of the air gap near the pole tips. The bigger the separation, the weaker the field. In fact, *any* air gap in the main flux path will strongly affect the B field because $\mu_r^{core} \gg \mu_r^{air} = 1$. For example, if $\mu_r^{core} = 1000$, introducing a 100 [μm] gap in a toroidal core 3 [cm] in diameter will approximately halve any induced B field. This has serious implications for the core design, where uniformity of performance of the four poles is important. It is therefore important that the design avoid spurious air gaps; or if they cannot be avoided, that they be controlled for uniformity.

While high μ_r^{core} is important, even more important is high core saturation B_{sat}^{core}. This is because we are trying to funnel as much flux as possible through the tapered pole to exit at the tip. For a given total flux Φ_m, the flux density B varies inversely with the core area. For high flux, it will exceed B_{sat}^{core} at some place in the taper where the area gets too small. The flux density at the tip is limited by B_{sat}^{core}. Excess flux escapes from the sides of the taper in the saturated parts of the tip. Increasing the MMF merely moves the saturation point back up the taper.

The highest saturation materials available are vanadium permendur and hiperco, both of which are not only expensive, but extremely difficult to fabricate. A good compromise is ASTM A 848 Magnet Iron which saturates at about 1.6 [T].

Complicating things even further, these desirable core materials are electrically conductive metals which means, according to Faraday's law $\nabla \times \boldsymbol{E} + \partial \boldsymbol{B}/\partial t = 0$, changes in B induce voltage gradients and consequently cause eddy currents in the core. The more rapid the change, the greater the current. This limits the bandwidth over which the core is operational. For the design in question, the bandwidth is in the low tens of Hertz, essentially DC. Accordingly, and to forestall false expectations, this design is called, a "DC Prototype."

Conventional methods of reducing eddy currents are by laminating thin sheets of the material to make up the core, or to mix a powder of the material with a non-conductive binder and cast the core. Lamination offers possibilities which can be explored, but powders rarely approach either the permeability or saturation properties of the base material.

Another possibility is a class of materials called "Metglas." These materials are metals formed as an amorphous rather than a crystalline solid by a process of hyperfast chilling of the metal from the molten state. Magnetic alloys such as mumetal are commercially produced as metglas with very good properties. Whether or not high saturation metglas materials can be obtained I do not know.

While not properly an issue for the DC prototype, this problem will have to be addressed if this design is to be developed for higher bandwidths.

2.3 Coil considerations

Looking at the concept picture on page 3, it is evident that the coils are awkward. Not only must they be tapered in the front, but how they will fit within the magnetic shell (which is conveniently not shown) is problematical. Add to this the need for lots of ampere turns in a limited conductor cross section, and the fact that winding coils with steeply conical end profiles is exceedingly difficult, it becomes apparent that this geometry leaves a lot to be desired.

This problem was addressed by moving the coils elsewhere. Considering a magnetic circuit model of the magnetic paths, each pole can be modeled as a MMF (depicted as overlapping circles in the figure) induced by the current in its coil, in series with a reluctance (depicted by the resistor symbol, or zigzag line) partially due to the pole core itself, but mostly incurred at the air gap between the pole tip and the location of the bead. The topology of the conceptual design consists of two nodes (depicted as ∘s) representing the magnetic shell and the bead respectively, connected by four arcs representing the four poles.

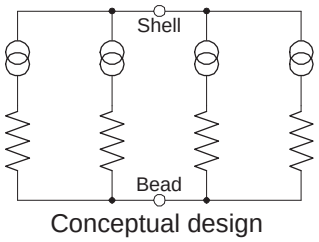

Conceptual design

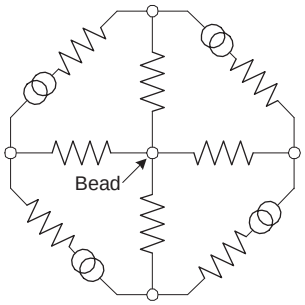

As built design

This topology can be extended by replacing the shell node by four back end nodes, each representing the back end of a pole, and by moving the MMFs from the pole arcs to the arcs connecting the back end nodes. In this topology, each pole is driven by two MMFs in parallel. The reluctances shown in series with each MMF those of the cores connecting the back end nodes and are small relative to the pole reluctances. Thus to a first approximation the effective MMF driving a pole is the average of the MMFs connected to its back end node. To the extent that the MMFs differ, they cause flux to circulate in the ring connecting the back end nodes.

This topology allows considerable flexibility in choice of the geometry used to implement it. As shown in Sheet 1 of the drawings in Appendix C, the coils were chosen to be easily wound on cylindrical bobbins with copious cross sectional area to allow for large Ampere turns.

2.4 A potential but probably not serious degeneracy

So called parasitic imperfections incurred by using real components which are only imperfectly represented by simple circuit models are often the cause of engineering headaches. They rarely work to one's advantage. However in this case, they probably do. In particular, they probably remove a mathematical degeneracy.

That is, we chose four poles as the minimum number to provide forces in full three dimensions. But the idea that the pole strengths sum to zero is a constraint that nullifies one degree of freedom. You can appreciate this if you try to find a set of drive currents that will pull the bead in a direction exactly half way between two poles, or to a direction opposite one of the poles.

The circuit models of the previous section enforce the concept of zero net flux from the four pole tips; or in other words, the sum of the strengths of the approximated monopoles

is zero. In fact, there are significant parasitic reluctances not shown due to leakage flux between various parts of the cores connecting the back end nodes and parts of the pole cores themselves. These parasitics mitigate the effects of the bothersome constraint. It remains to be seen how effective this reprieve will be.

References

[Amblard96] François Amblard, B.Y. Pargellis, A. Pargellis, S. Leibler, "A magnetic manipulator for studying local rheology and micromechanical properties of biological systems," *Review of Scientific Instruments,* v.67 no.3, March 1996, pp818-827.

[Bausch98] Andreas R. Bausch, F. Ziemann, A. A. Boulbitch, K. Jacobson, E. Sackmann, "Local Measurements of Viscoelastic Parameters of Adherent Cell Surfaces by Magnetic Bead Rheometry," *Biophysical Journal,* v.75, October 1998, pp2038-2049.

[Bausch99] Andreas R. Bausch, W. Möller, E. Sackmann, "Measurement of Local Viscoelasticity and Forces in Living Cells by Magnetic Tweezers," *Biophysical Journal,* v.76, January 1999, pp573-579.

[Haber00] Charbel Haber, D. Wirtz, "Magnetic Tweezers for DNA micromanipulation," *Review of Scientific Instruments,* v.71 no.12, December 2000, pp4561-4570.

[Jackson62] J. D. Jackson, "Classical Electrodynamics," John Wiley & Sons, New York, 1962.

Appendix A: Force on a soft magnetic bead in a magnetic field

NOTE: the original derivation was erroneous and is here corrected

According to [Jackson62], the magnetization induced in a permeable sphere by an applied external field $\boldsymbol{B}$ is

$$\boldsymbol{M} = \frac{3}{4\pi}\left(\frac{\mu - 1}{\mu + 2}\right)\boldsymbol{B}, \qquad \text{(J :5.115)}^{\dagger}$$

in Gaussian units. From Jackson's *Appendix on Units and Dimensions,* we convert to SI units according to $M \rightarrow M\sqrt{\mu_0/4\pi}$, $B \rightarrow B\sqrt{4\pi/\mu_0}$, and $\mu \rightarrow \mu/\mu_0$, obtaining

$$\boldsymbol{M} = \frac{3}{\mu_0}\left(\frac{\mu_r - 1}{\mu_r + 2}\right)\boldsymbol{B}, \qquad (A.1)$$

where $\mu_r = \mu/\mu_0$ is the relative permeability inside the sphere.

To obtain the magnetic dipole moment $\boldsymbol{m}$ of the sphere, we integrate $\boldsymbol{M}$ over its volume. Since the magnetization $\boldsymbol{M}$ inside the sphere is uniform, the integral is simply the volume of the sphere times $\boldsymbol{M}$, or

$$\boldsymbol{m} = \frac{\pi d^3}{2\mu_0}\left(\frac{\mu_r - 1}{\mu_r + 2}\right)\boldsymbol{B}. \qquad (A.2)$$

Again from Jackson, the force on a magnetic moment $\boldsymbol{m}$ in a magnetic field $\boldsymbol{B}$ is,

$$\boldsymbol{F} = \nabla \times (\boldsymbol{B} \times \boldsymbol{m}) = (\boldsymbol{m} \cdot \nabla)\boldsymbol{B} = \nabla(\boldsymbol{m} \cdot \boldsymbol{B}) \qquad \text{(J :5.69)}$$

Substituting eq(A.2) into eq(J: 5.69):

$$\boldsymbol{F} = \frac{\pi d^3}{2\mu_0}\left(\frac{\mu_r - 1}{\mu_r + 2}\right)\nabla(B^2). \qquad (A.3)$$

†Equation numbers prefixed by "J:" are from [Jackson62].

Appendix B: Parametric simulations of monopole configurations

A parametric study of the monopole model was conducted with Matlab code. The model consists of a magnetic bead located at the origin, a "driven" monopole of strength Q on the z-axis at $z = z_0$, and n "return" monopoles of strength $-Q/n$ arranged equally spaced around a circle of radius r coaxial with z and located at $z = z_c$. For $n = 3$, $r = 0.9428$, $z_c = -z_0/3$, this model represents an equilateral tetrahedral pole geometry.

Using the function Fcoax(), it was first determined that for $2 \leq n \leq 20$, the force was independent of n, demonstrating no advantage in force from a larger number of poles.

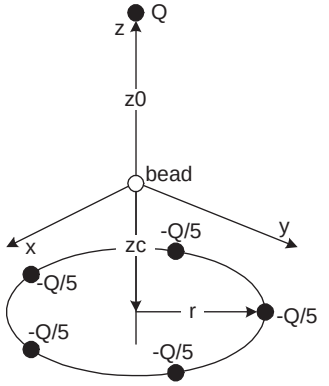

Example geometry, n=5

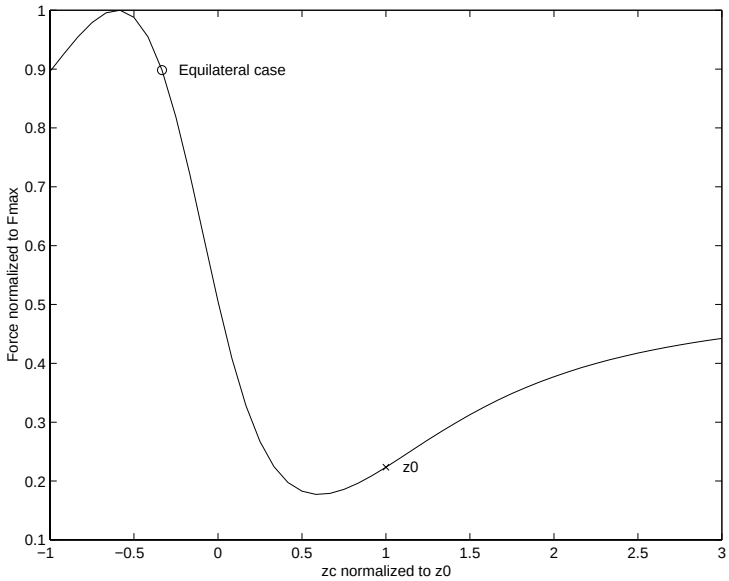

The function parametric() was then constructed to investigate the force behavior of non equilateral tetrahedra of the kind modeled. A plot of normalized force as a function of position zc shows that the equilateral tetrahedron produces 89.8% of the maximum force, which occurs for a slightly elongated tetrahedron from equilateral.

Matlab codes are included next. Fcoax() is the function that calculates a single instance of the bead force. Parametric() makes a plot of bead force while varying z_c.

```
function F = Fcoax(Q, n, z0, r, zc, chi, a)
% Fcoax(Q, n, z0, r, zc, chi, a) -- Calculate the force on a bead of
% radius a and susceptibility chi at the origin exerted by n poles
% positioned coaxially about the z axis at z = zc, each with strength
% -Q/n, and one pole on the z axis at z = z0 with strength Q.

R = coax(z0, r, zc, n);
for i = 1:n
    q(i) = -Q/n;
end
q(n+1) = Q;
F = Fbead(q, R, chi, a);
```

```
function parametric(n)
% parametric(n) -- Calculate the force at the origin as zc is varied.
% Let the dominant pole be located at z0 = 1, and zc be the location
% of the center of a circle coaxial with z.  Report the position zm
% of the maximum force Fm, and the percentage force 100*Ft/Fm at
% zt = -1/3 which represents an equilateral tetrahedron (circle radius
% of 0.9428).  Generates a normalized plot of F(z) where "x" marks
% position of the main pole, and "o" marks the tetrahedral case.

n = 2*fix(n/2)+1; % ensure n is odd
s = 1;
D = 2;
z = linspace(s-D,s+D,n);
for i = 1:n
    F(i,:)  = Fcoax(1, 3, s, 0.942809041582, z(i),1000,1.0e-7);
    if abs(z(i)-s) < D/(n-1)
        zs = i;
    end
    if abs(z(i)+s/3) < D/(n-1)
        zc = i;
    end
    if i == 1
        Fmax = F(i,1);
    else
        if F(i,1) > Fmax
            Fmax = F(i,1);
            imax = i;
        end
    end
end
plot(z, F(:,1)/Fmax, 'k',...
    z(zc), F(zc,1)/Fmax, 'ko',...
    z(zs), F(zs,1)/Fmax, 'kx');
xlabel('zc normalized to z0');
ylabel('Force normalized to Fmax');
text(z(zc)+0.1, F(zc,1)/Fmax, 'Equilateral case');
text(z(zs)+0.1, F(zs,1)/Fmax, 'z0');
zmax = z(imax)
percent = F(zc,1)/Fmax
```

```
function p = coax(z0, r, zc, n)
% coax(z0, r, zc, n) -- generate n points on a circle of radius r coaxial
% with z, located z = zc from the origin, and one point at [z0,0,0].

dphi = 2*pi/n;
for i = 1:n
    phi = i*dphi;
    p(i,:)  = [zc, r*sin(phi), r*cos(phi)];
end
p(n+1,:)  = [z0, 0, 0];
function F = Fbead(q, R, chi, a)
% Fbead(q, R, chi, a) -- Force on a spherical bead of susceptibility chi
% and radius a, located at the origin, exerted by magnetic poles of
% strengths q located at locations R.

B = sum(Bfield(q, R),1);
dB = sum(GradB(q, R),1);
F = (4*pi*a^3/3)*chi*dot(B, dB)*B/norm(B);
```

```
function B = Bfield(q, R)
% Bfield(q, R) -- N magnetic induction vectors B at the origin induced
% by N magnetic poles of strength q at locations R. [SI units]
% q is a 1:N list of pole strengths, R is an N:3 matrix of N vectors R.

if length(q)  = length(R(:,1))
    error('Number of poles q inconsistent with number of locations R.');
end
for i = 1:length(R(:,1))
    B(i,:)  = q(i)*R(i,:)/(4*pi*norm(R(i,:))^3);
end
```

```
function Gb = Gradb(q, R)
% gradB(q, R) -- Gradient of scalar B-field strength b at the origin,
% contributed by a pole of scalar strength q at vector location R.
% [SI units]

% Notation:
% Let Du_v be the total derivative of u wrt v, and du_v be the partial
% derivative.  Let w represent a scalar, W represent a vector, and W^
% represent a unit vector.
%
% The scalar Db_r is the magnitude of the gradient vector DB_r which
% points along the unit vector R^. Thus the directional derivatives
% of b along the coordinate axes can be written,
% x^db_x = x^Db_r*dr_x, and similarly for y, and z.
% Thus, grad*b = Db_r*grad*r = Db_r*R/r.
% q is a 1:N list of pole strengths, R is an N:3 matrix of N vectors R.

if length(q)  = length(R(:,1))
    error('Number of poles q inconsistent with number of locations R.');
end
for i = 1:length(q)
    r = norm(R(i,:));
    gradr = -R(i,:)/r; % Negative because direction is towards the origin.
    dbdr = -q(i)/(2*pi*r3^);
    Gb(i,:)  = dbdr*gradr;
end
```

Appendix C: Specification of the Magnets

This appendix contains the shop drawings specifying the materials and construction of the DC prototype magnet assembly.

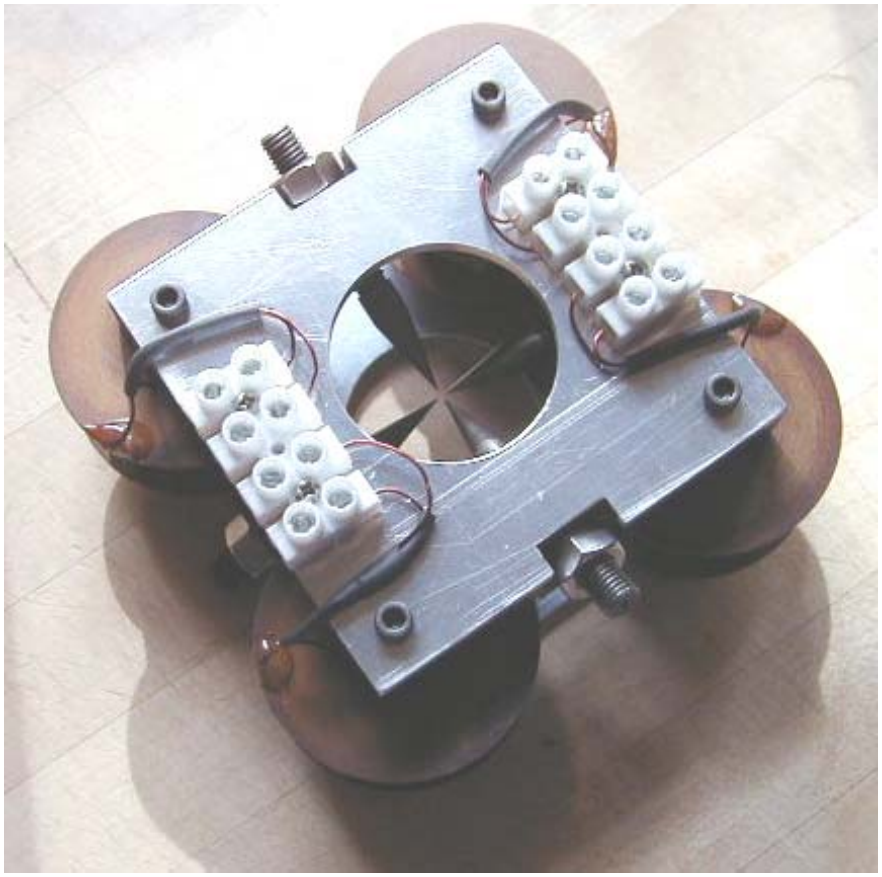

To the best of my knowledge, the included drawing revisions are the current as-built prototype configuration. Please note the drawings are in units of [cm] – the choice seemed well motivated at the time, but after working with the instrument makers in the Physics Machine Shop, I think I'd do it in inches next time.

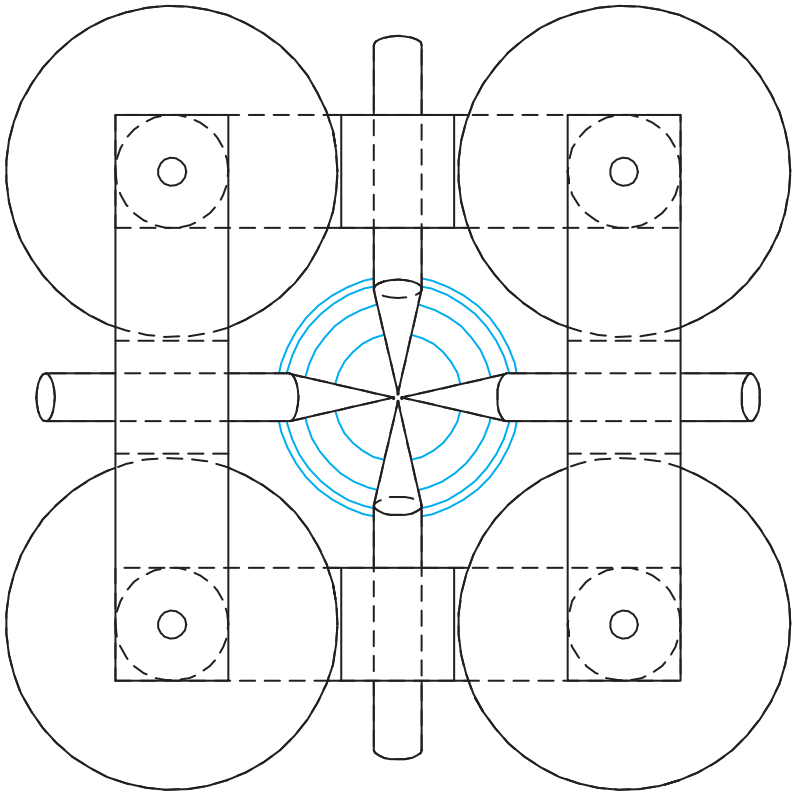

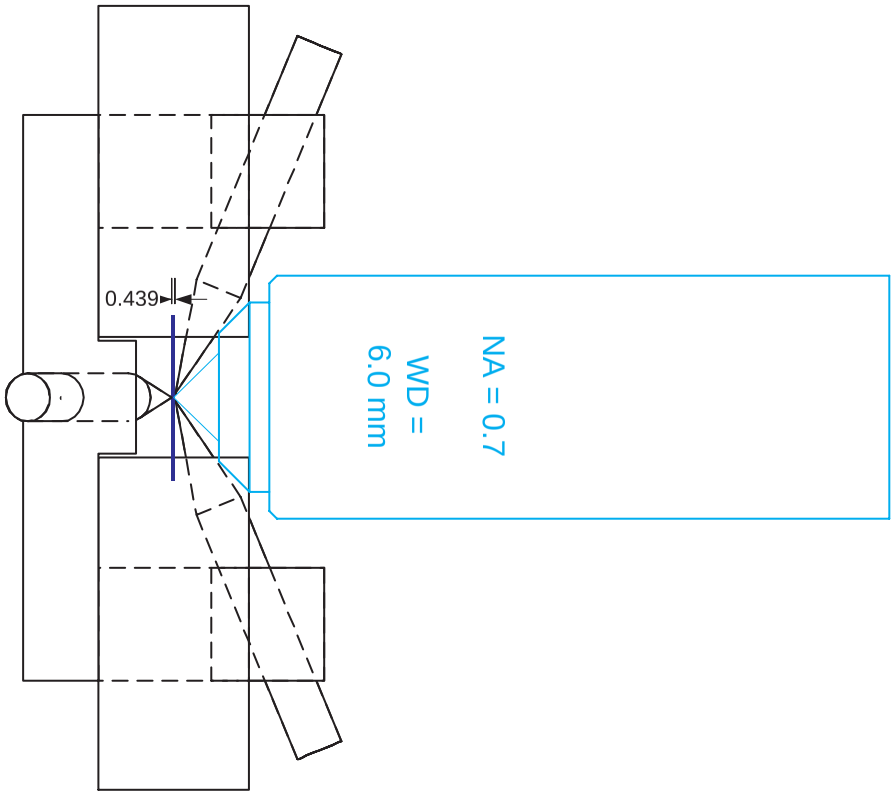

Sample stage thickness is 439u; allow 450u vertical clearance between tips..
The core angles are 22.5 degrees, so each is backed out (450u/2)/tan(22.5) = 543u in the XY plane.

Magnetic components only shown in black, sample stage in blue, optical lens, shown on bottom side only, in aqua. Other mechanicals not shown include top and bottom plates, clamping fastners, and adjustment-locking jam nuts.

MSL	TITLE	3DFM			
	DESCRIPTION	DC prototype Magnet Assembly			
DRAWN BY Leandra Vicci	SIZE	DWG NO	Magnet 1.0		
DATE 20 February 2001	A	SCALE 1: 1	REV 1	SHEET 1 OF 8	

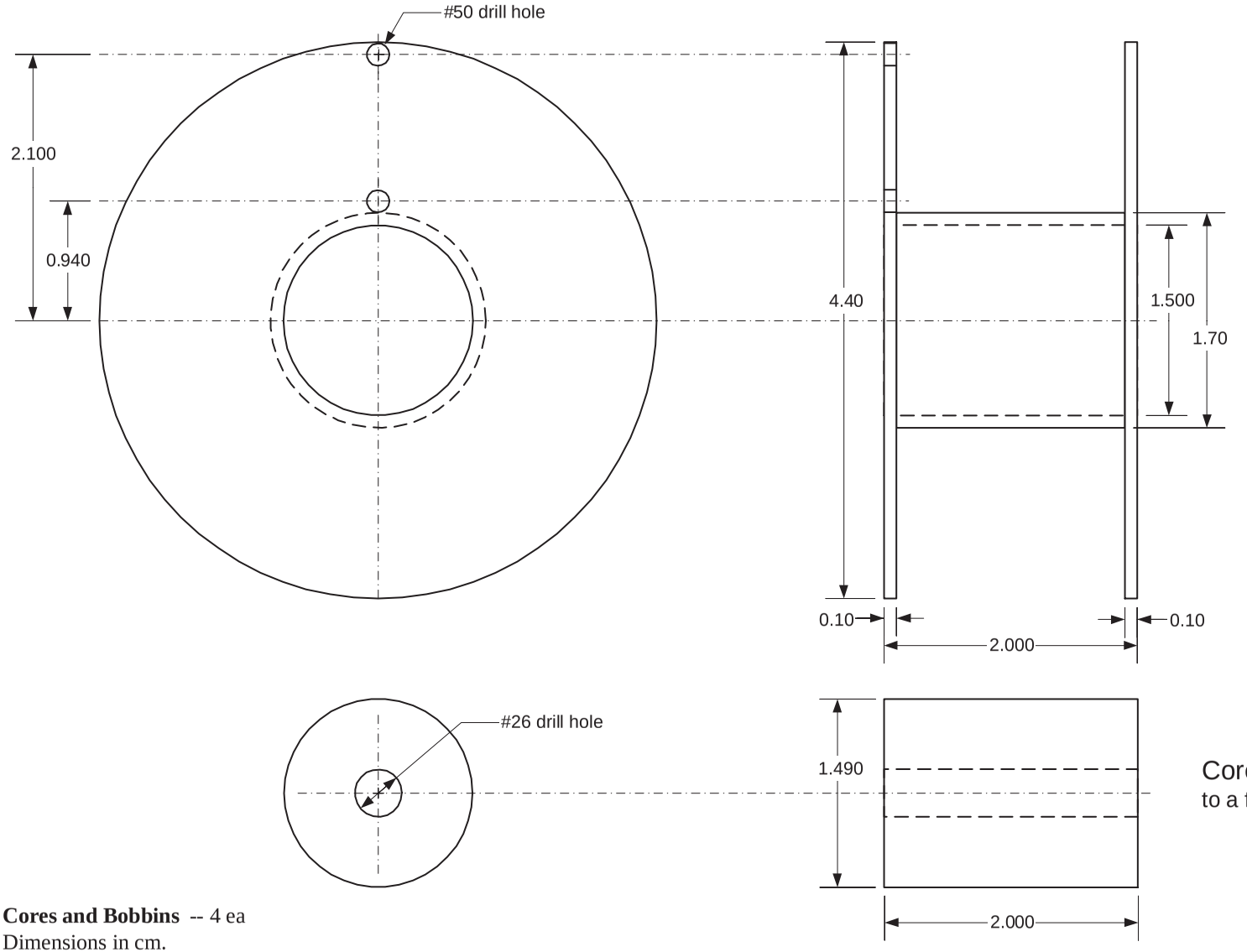

Cores and Bobbins -- 4 ea
Dimensions in cm.
Tolerances, except where noted otherwise --
for dimensions shown to 2 places: +/- 0.01cm,
for dimensions shown to 3 places: +/- 0.004cm.

Core material ASTM A848 Type 1 Low Carbon Magnetic Iron. Protect from oxidation during fabrication, finish with blueing process (ferrous oxide) until visibly black, then lightly oil.

Bobbin material: phenolic composite.
Bobbin to core clearance nominally class RC7.

Coil specifications:

Wind 14 full layers, (about 340 turns) of #22AWG formvar insulated magnet wire. The number of turns and direction of winding shall be the same for all four coils

MSL	TITLE: 3DFM					
	DESCRIPTION: DC prototype Coil Core and Bobbin					
DRAWN BY: Leandra Vicci	SIZE: A	DWG NO: Magnet 1.1				
DATE: 16 March 2001		SCALE: 2: 1	REV: 1.3	SHEET: 2 OF 8		

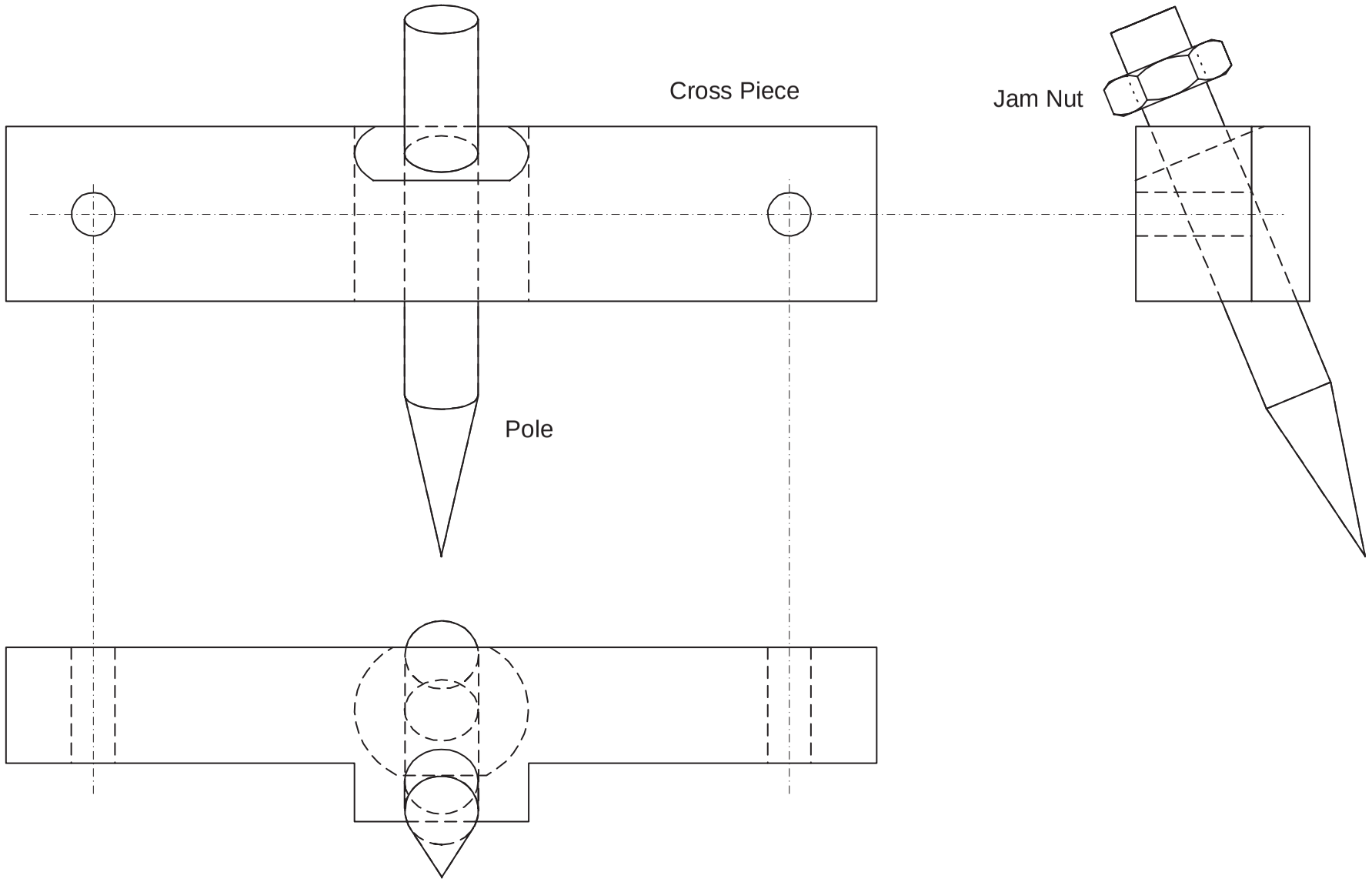

MSL	TITLE: 3DFM				
	DESCRIPTION: DC prototype Magnetic Pole and Cross Piece Assemb				
DRAWN BY: Leandra Vicci	SIZE: A	DWG NO: Magnet 1.2			
DATE: 20 February 2001		SCALE: 2: 1	REV: 1	SHEET: 3 OF 8	

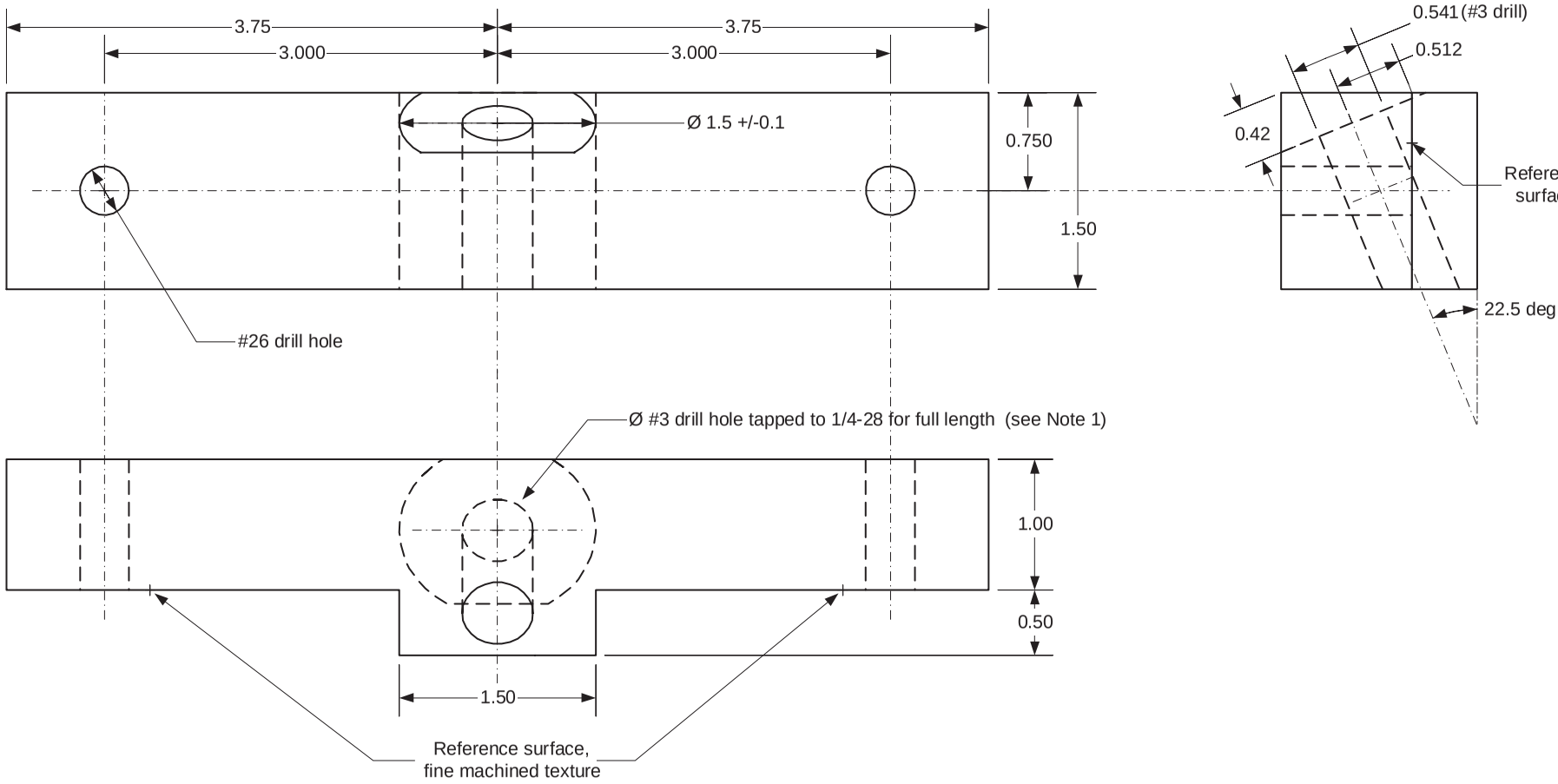

Magnetic cross pieces -- 4 ea.

Material is ASTM A848 Type 1 Low Carbon Magnetic Iron
Dimensions in cm.
Tolerances, except where noted otherwise --
for dimensions shown to 2 places: +/- 0.01cm,
for dimensions shown to 3 places: +/- 0.004cm.
angular: +/- 0.1 degrees, but *variation between pieces to be less than 0.01 degrees* .

Protect from oxidation during fabrication, finish with blueing process (ferrous oxide) until visibly black, then lightly oil.

Note 1: Hole drilling and threading operations to be precisely aligned.

MSL	TITLE	3DFM			
	DESCRIPTION	DC prototype Magnetic Cross Piece			
DRAWN BY Leandra Vicci	SIZE	DWG NO	Magnet 1.2.1		
DATE 16 March 2001	A	SCALE 2: 1	REV 1.2	SHEET 4 OF 8	

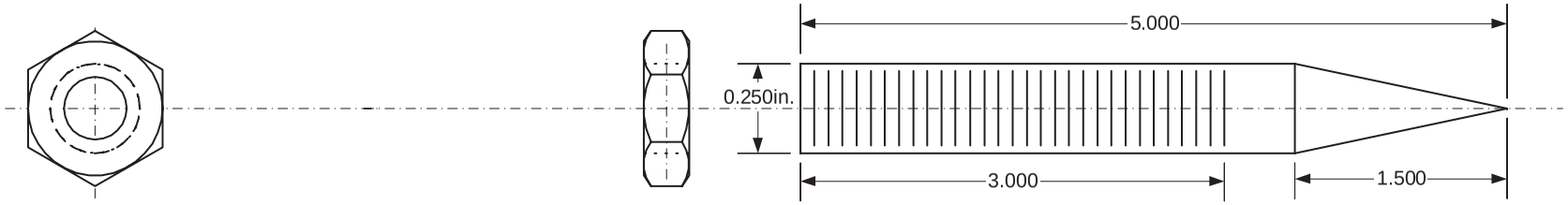

Poles -- 4 ea.
Jam nuts -- 12ea

Dimensions in cm.
Tolerances: +/- 0.004cm.

Pole material is ASTM A848 Type 1 Low Carbon Magnetic Iron,
Pole threaded 1/4-28 NF for 3cm.
Pole uniformly tapered for 1.5cm to a point not exceeding 0.005cm diameter.
Protect pole from oxidation during fabrication, finish with blueing process (ferrous oxide) until visibly black, then lightly oil.

Jam nut is 1/4-28 NF.
Material is brass or non-magnetic stainless steel.

MSL	TITLE: 3DFM				
	DESCRIPTION: DC prototype Magnetic Poles and Jam nuts				
DRAWN BY: Leandra Vicci	SIZE: A	DWG NO: Magnet 1.2.2			
DATE: 20 February 2001		SCALE: 2: 1	REV: 1	SHEET: 5 OF 8	

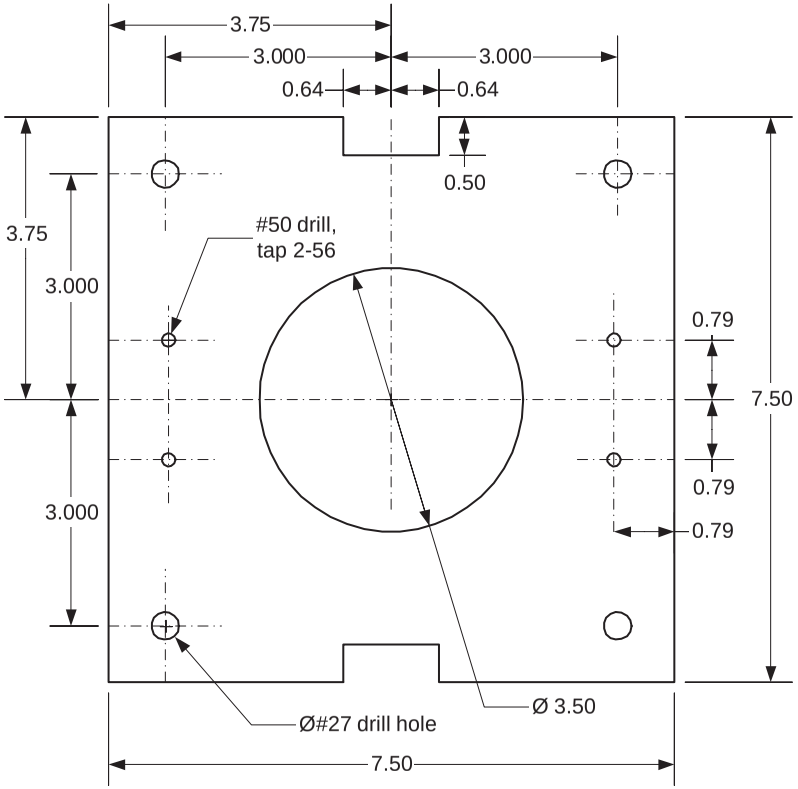

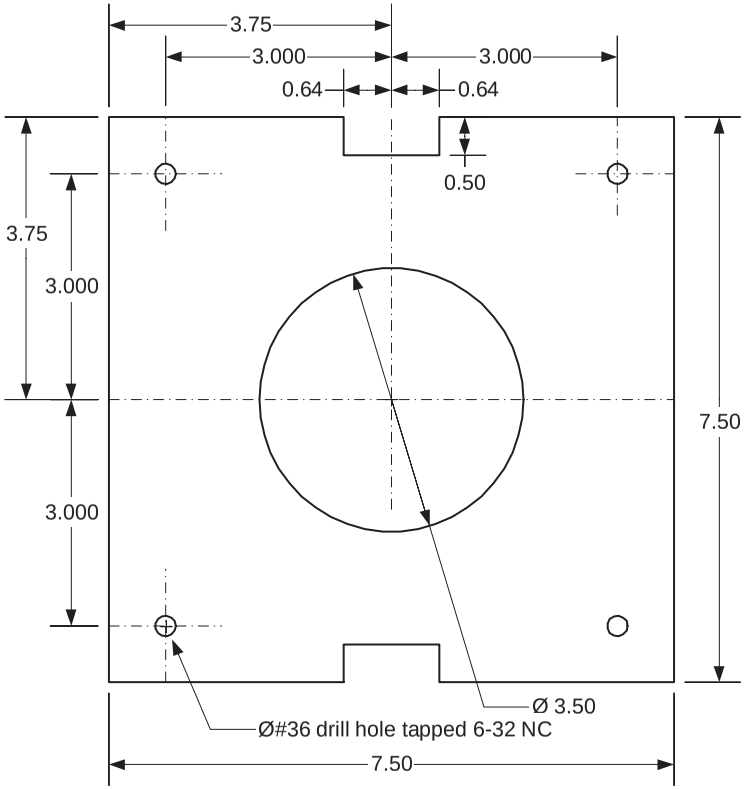

Top Plate -- 1ea

Dimensions in cm.
Tolerances,
for dimensions shown to 2 places: +/- 0.01cm,
for dimensions shown to 3 places: +/- 0.004cm.

Material: 1/8 inch 2024 Aluminum or equivalent

Terminal blocks (not shown): Beau Interconnect, 4 pole, type C1504-151, stock no. 89F5990; 2ea.

Bottom Plate -- 1ea

Dimensions in cm.
Tolerances,
for dimensions shown to 2 places: +/- 0.01cm,
for dimensions shown to 3 places: +/- 0.004cm.

Material: 1/8 inch 2024 Aluminum or equivalent

MSL	TITLE	3DFM				
	DESCRIPTION	DC prototype Mounting plates				
DRAWN BY Leandra Vicci	SIZE	DWG NO	Magnet 1.3			
DATE 16 March 2001	A	SCALE 1: 1	REV 1.2	SHEET 6 OF 8		

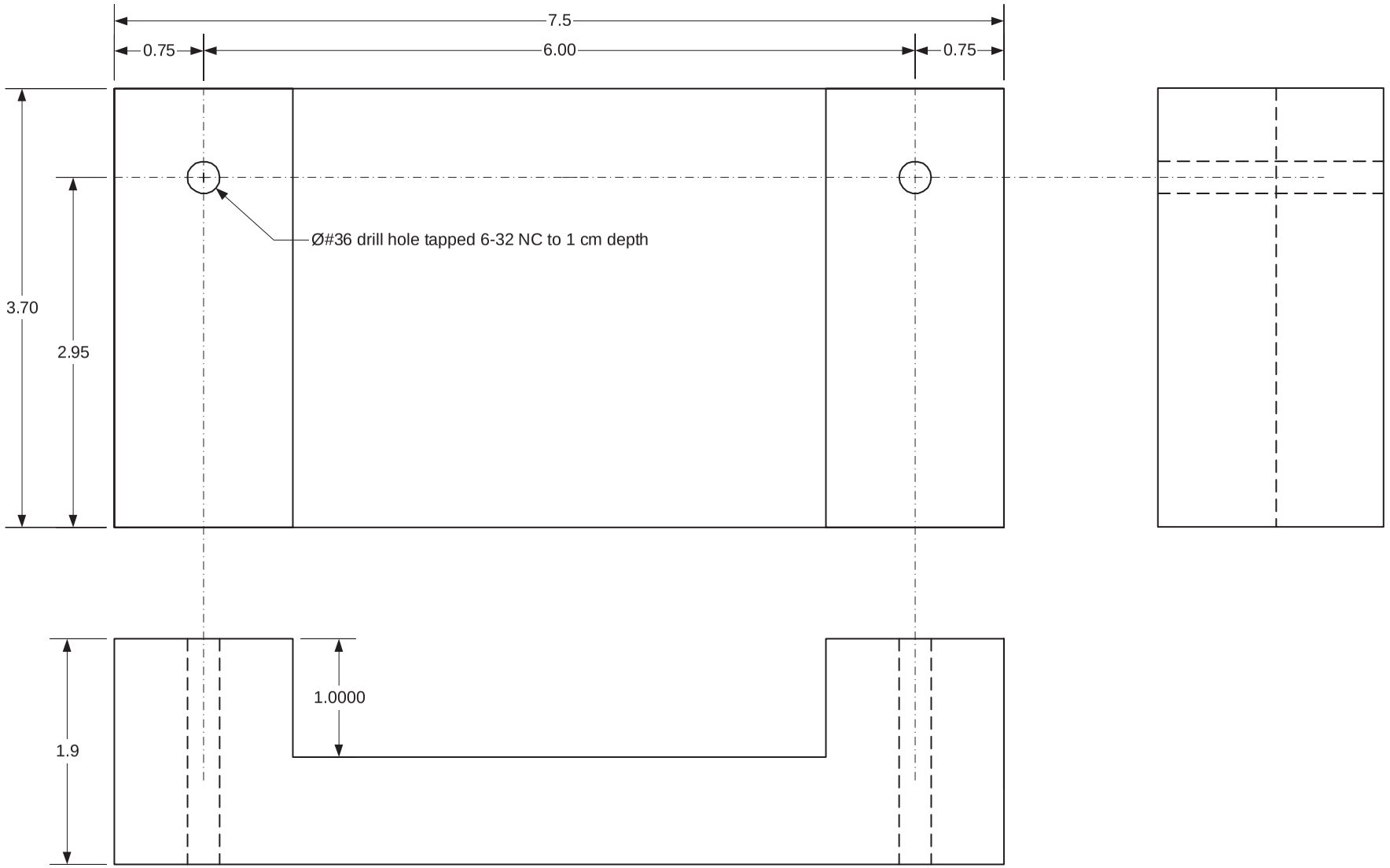

Z Alignment Jig -- 1ea

Dimensions in cm.
Tolerances,
for dimensions shown to 1 place: nominal
for dimensions shown to 2 places: +/- 0.01cm,
for dimensions shown to 4 places: as accurate as you can make it.

Material: 3/4 inch 2024 Aluminum or equivalent

MSL	TITLE	3DFM				
	DESCRIPTION	DC prototype Z Alignment Jig				
DRAWN BY Leandra Vicci	SIZE	DWG NO	Magnet 1.4			
DATE 7 March 2001	A	SCALE 2: 1	REV 1.2	SHEET 7 OF 8		

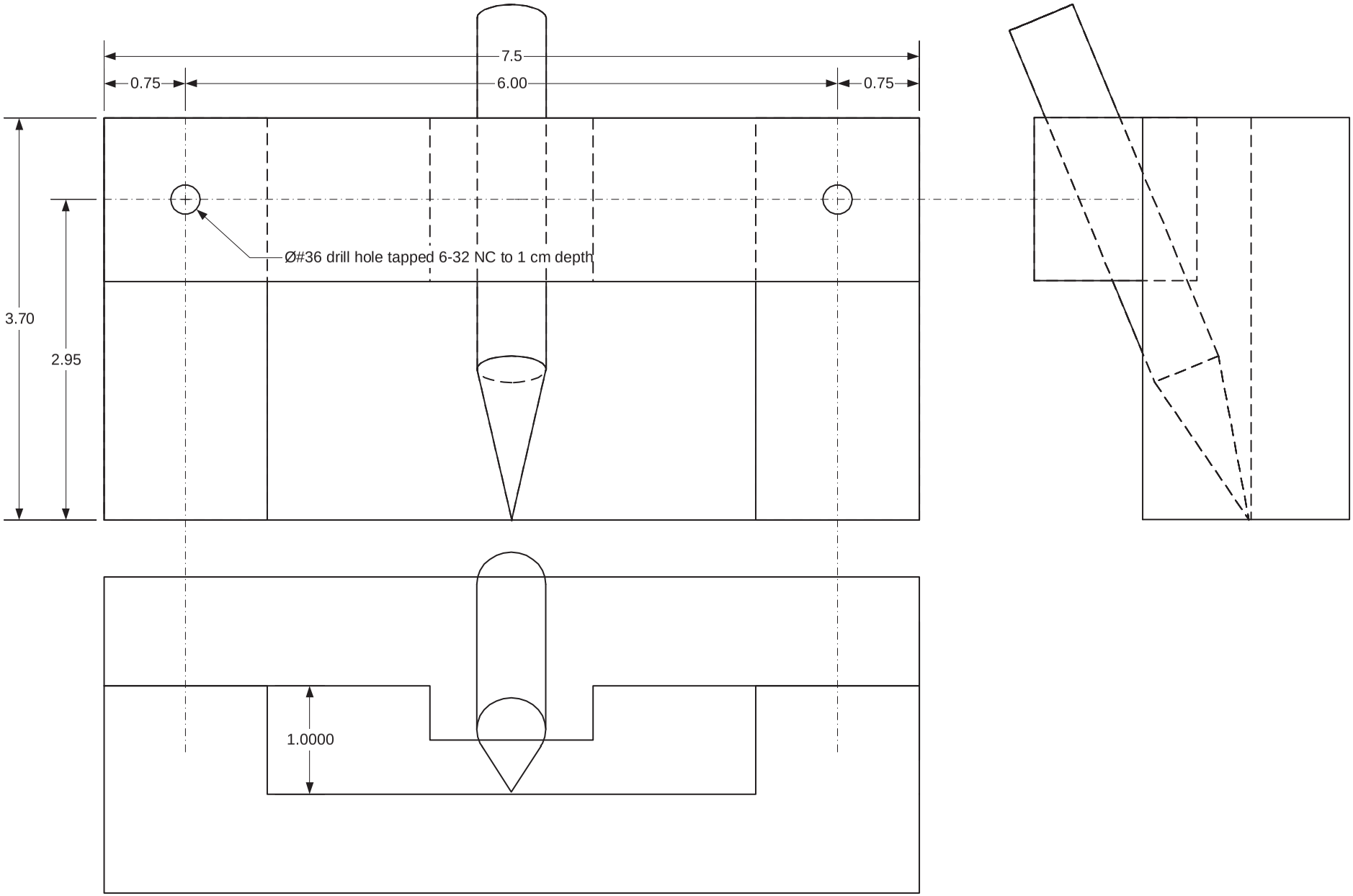

Z Alignment Jig usage

Mount magnetic cross piece and core
assembly with jam nuts,
torque mounting screws to spec,
adjust core for Z tip clearance clearance
shown, using microscope and reticle,
lock core adjustment with jam nut.

MSL	TITLE: 3DFM				
	DESCRIPTION: DC prototype Z Alignment Jig usage detail				
DRAWN BY: Leandra Vicci	SIZE: A	DWG NO: Magnet 1.4.1			
DATE: 7 March 2001		SCALE: 2: 1	REV: 1.1	SHEET: 8 OF 8	

Appendix D: Specification of the Drive Electronics

This appendix contains the shop drawings specifying the parts and construction of the DC prototype magnet drive electronics. The drawings do not show the as-built ventilation holes in the top and bottom of the enclosure and rubber feet to provide bottom clearance. These were added to provide better cooling for the power supplies contained in the box.

If I were to design this again, I would forego the grounded-load circuit topology of the transconductance amplifiers. As built, even with significant debug effort, small oscillations in the MHz range still occur under certain operating conditions. While these do not apparently cause distortion of the transconductance gain at low frequencies, it is still not a desirable situation. My best guess is that floating the load (coil) and grounding the current sense resistor would provide a topology free of this problem. The cabling to the coils would support this topology without modification.

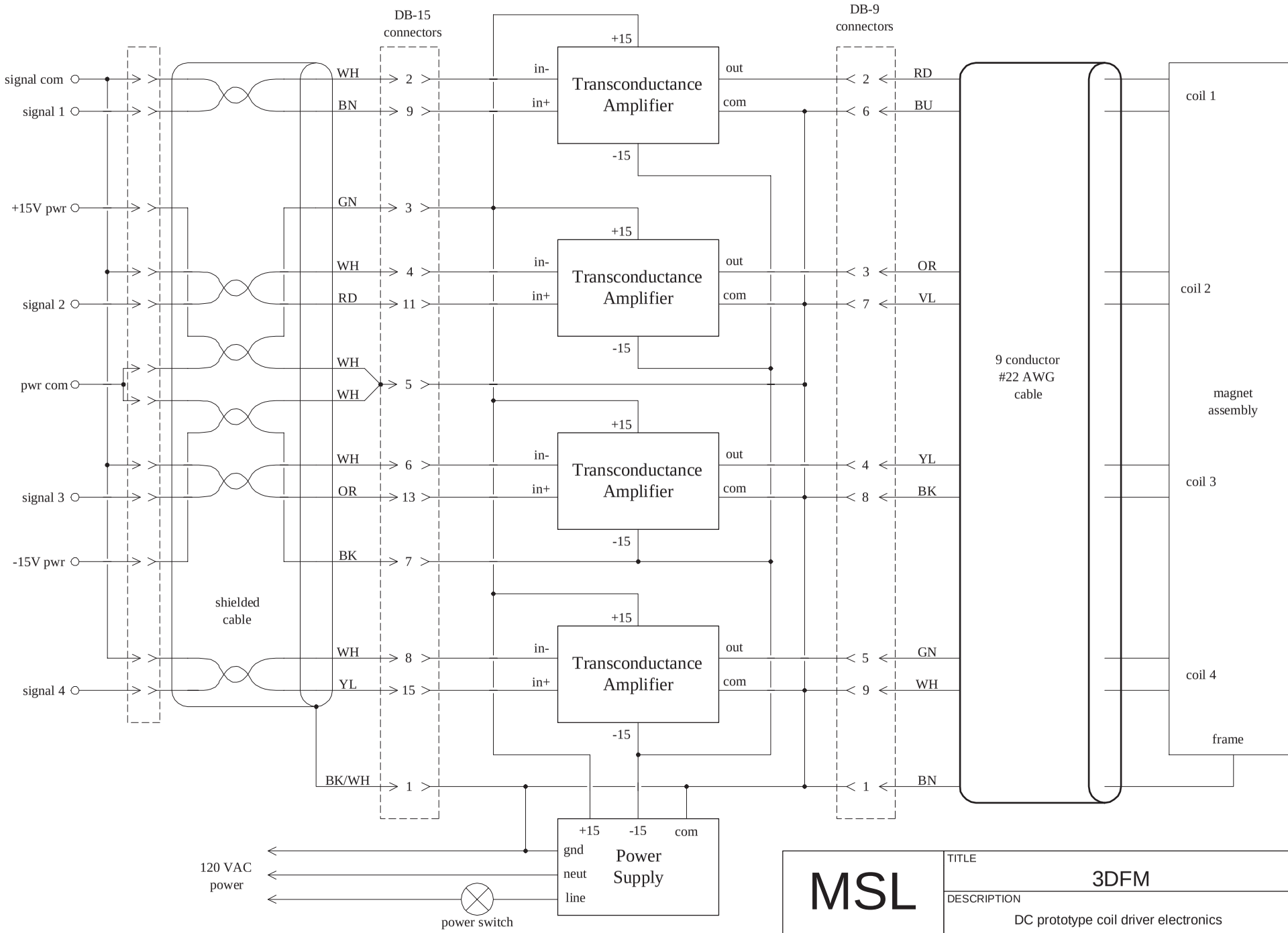

MSL	TITLE	3DFM			
	DESCRIPTION	DC prototype coil driver electronics			
DRAWN BY Leandra Vicci	SIZE	DWG NO	Driver 1.0		
DATE 9 May 2001	A	SCALE 1: 1	REV 1	SHEET 1 OF 13	

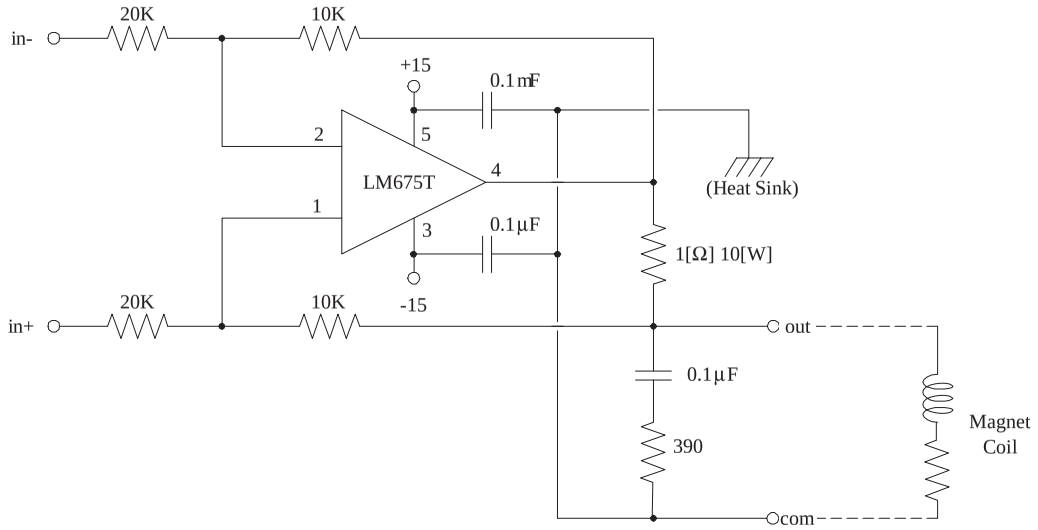

Coil driver transconductance amplifier, gain = 0.5 [A/V]. (4ea)

Slew rate limit approx 1200 [A/s] for a 10 [mH] coil.

All resistors 1%, metal film; except for a 1 [Ω] 10 [W] wire wound, Dale RH-10 1[Ω] 1%, Newark P/N 01F9597.

All capacitors are X7R ceramic, 50 [V] or equivalent.

All "ground" connections are to a common point close to the op amp package, and connected closely to the heat sink.

National Semiconductor LM675T power op amp (TO-220 case) to be insulated from heat sink by appropriate insulating washer and fastener.

MSL	TITLE: 3DFM			
	DESCRIPTION: DC prototype transconductance amplifier			
DRAWN BY: Leandra Vicci	SIZE: A	DWG NO: Driver 1.1.0		
DATE: 13 June 2001		SCALE: 1: 1	REV: 1	SHEET: 2 OF 13

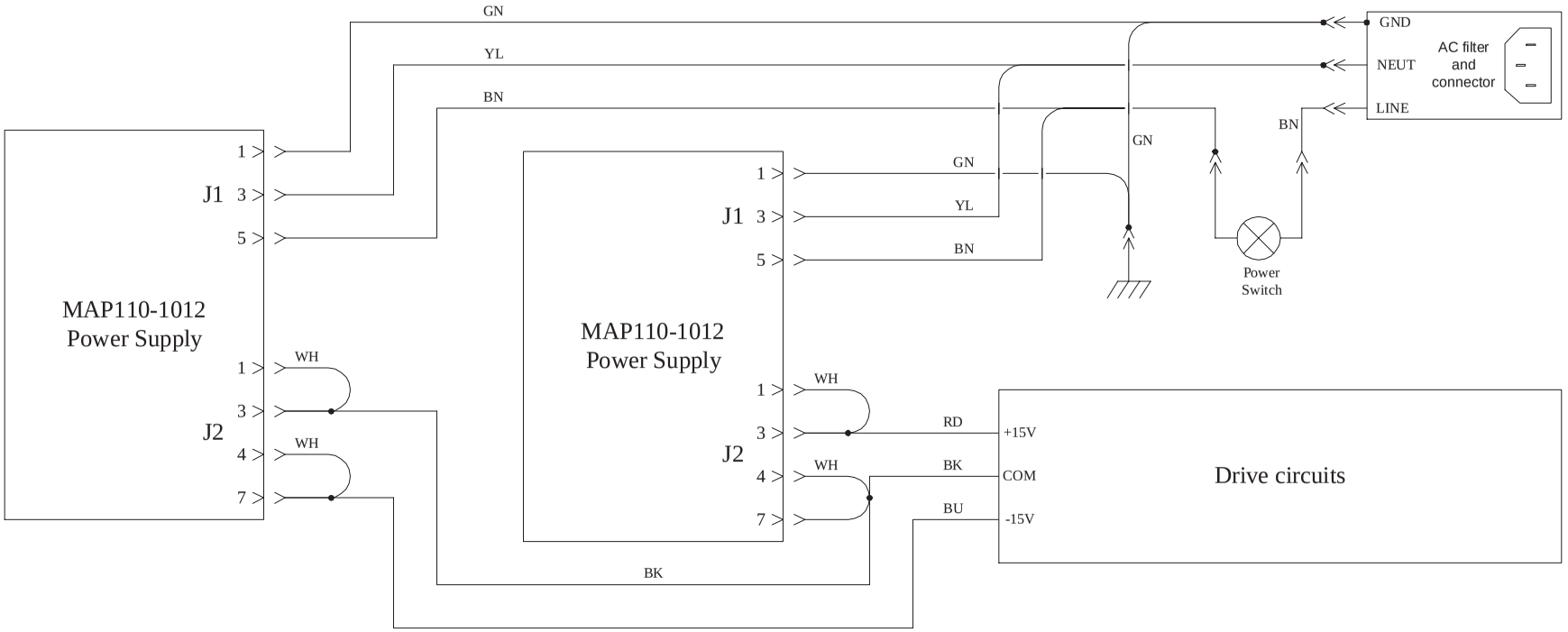

Power supplies: Power One MAP110-1012. (2ea)
Adjust V1 to 15 [V]. Each supply rated at 15[V]/8[A].

AC power harness mating with J1 uses Molex 09-50-3051-P shell
(Newark #44F4483) with Molex 08-52-0072-C pins (Newark #93F9690)

DC power harness mating with J2 uses Molex 09-50-3131-P shell
(Newark #94F9664) with Molex 08-52-0072-C pins (Newark #93F9690)

MSL		TITLE	3DFM			
		DESCRIPTION	DC prototype coil driver electronics power harness			
DRAWN BY	Leandra Vicci	SIZE	DWG NO	Driver 1.1.1		
DATE	13 June 2001	A	SCALE 1: 1	REV 1	SHEET	3 OF 13

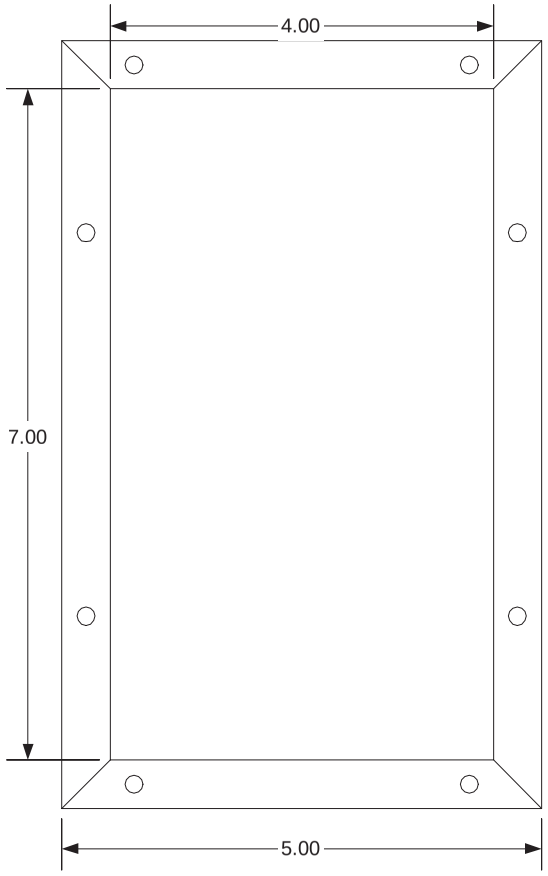

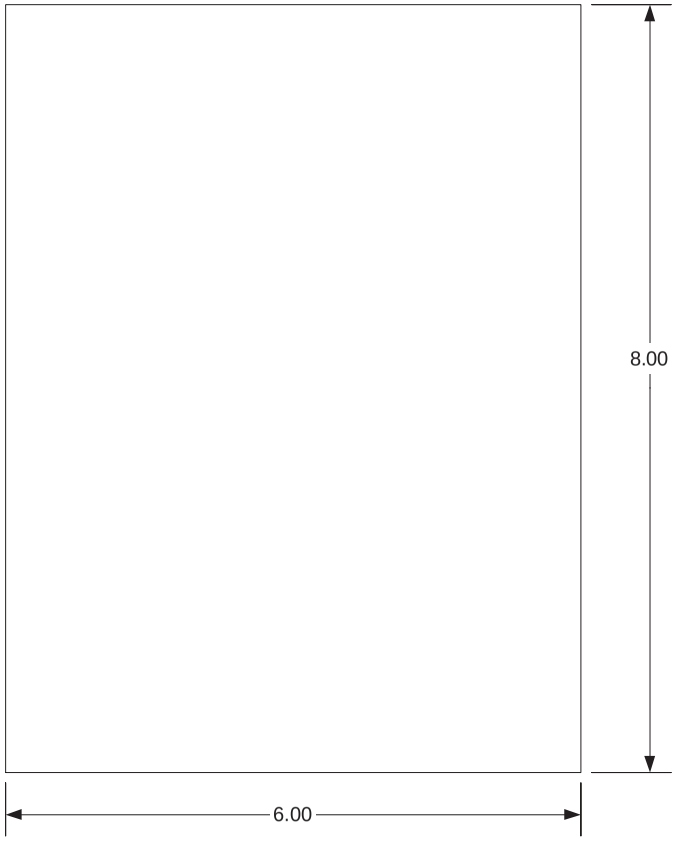

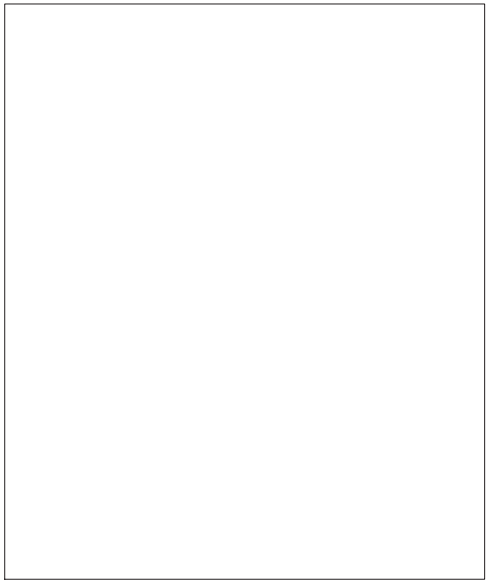

Drive electronics box. (1 ea)
Two pieces to be folded and TIG welded to make up the box.

MSL	TITLE: 3DFM					
	DESCRIPTION: DC prototype drive electronics box					
DRAWN BY: Leandra Vicci	SIZE: A	DWG NO: Driver 1.2				
DATE: 30 March 2001		SCALE: 1: 2	REV: 0	SHEET: 4 OF 13		

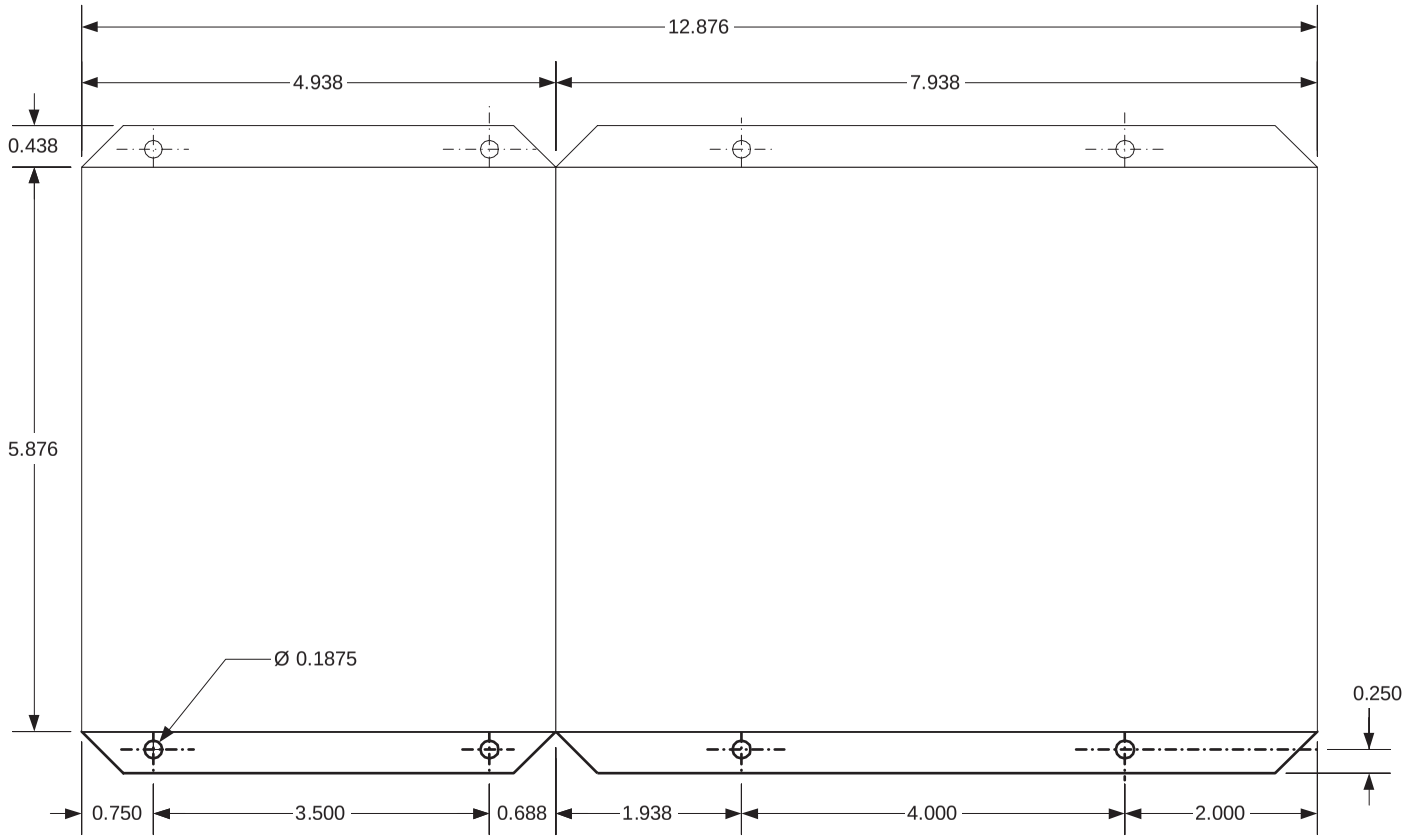

Pattern for drive electronics box. (2ea). Material: 0.064" 6061-0 Aluminum sheet.

Pattern is sized for fabrication with a bend radius of 1.5 x material thickness = 0.096".
The calculated bend allowance BA = 0.196" and the calculated setback SB = 0.160".
(Each leg is shortened by (SB - BA/2) = 0.062" for each fold to which it is adjacent)

MSL	TITLE: 3DFM				
	DESCRIPTION: DC prototype drive electronics box piece pattern				
DRAWN BY: Leandra Vicci	SIZE: A	DWG NO: Driver 1.2.1			
DATE: 30 March 2001		SCALE: 1: 2	REV: 0	SHEET: 5 OF 13	

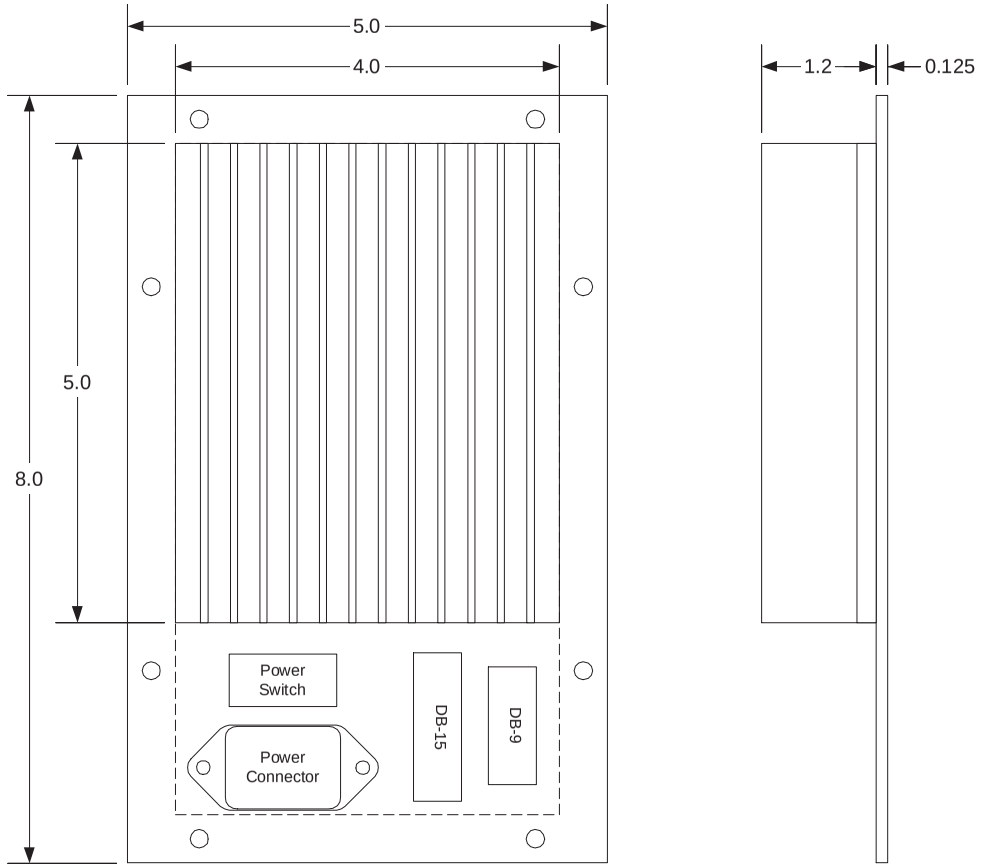

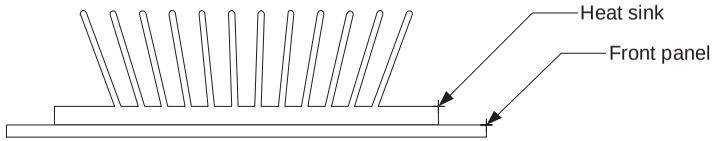

MSL	TITLE: 3DFM					
	DESCRIPTION: DC prototype drive electronics front panel assembly					
DRAWN BY: Leandra Vicci	SIZE: A	DWG NO: Driver 1.3				
DATE: 3 April 2001		SCALE: 1: 2	REV: 0	SHEET: 6 OF 13		

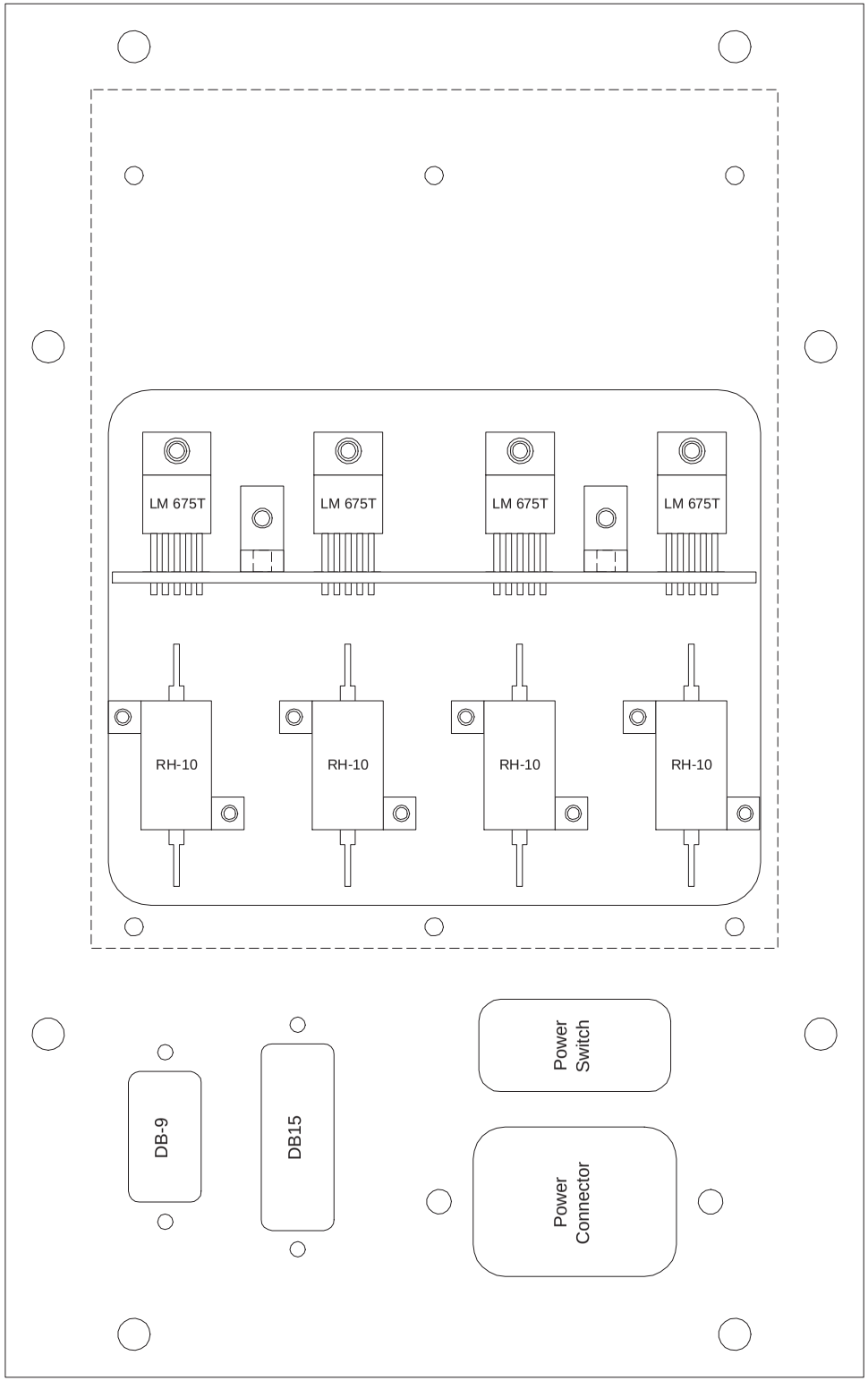

Rear view of front panel assembly with heat sink outline shown as a hidden line. The circuit board with its mounting brackets is shown along with the current sense resistors and power Op Amps.

MSL	TITLE: 3DFM				
	DESCRIPTION: DC prototype drive electronics, rear view of front panel assembly				
DRAWN BY: Leandra Vicci	SIZE: A	DWG NO: Driver 1.3.0			
DATE: 4 April 2001		SCALE: 1: 1	REV: 0	SHEET: 7 OF 13	

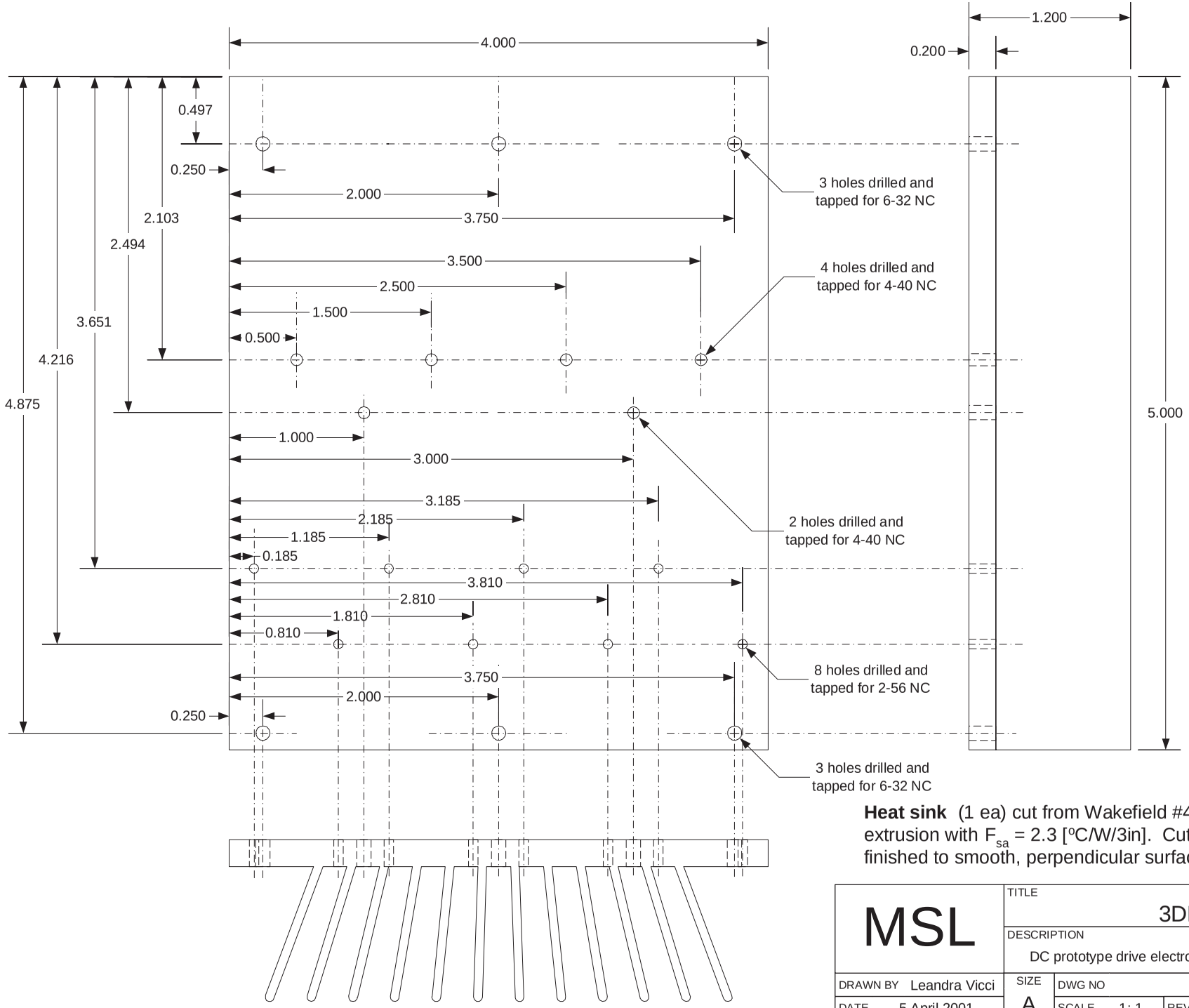

Heat sink (1 ea) cut from Wakefield #4678 aluminum extrusion with F_{sa} = 2.3 [ºC/W/3in]. Cut ends to be mill finished to smooth, perpendicular surfaces.

MSL	TITLE: 3DFM				
	DESCRIPTION: DC prototype drive electronics heat sink, rear view				
DRAWN BY: Leandra Vicci	SIZE: A	DWG NO: Driver 1.3.1			
DATE: 5 April 2001		SCALE: 1: 1	REV: 0	SHEET: 8 OF 13	

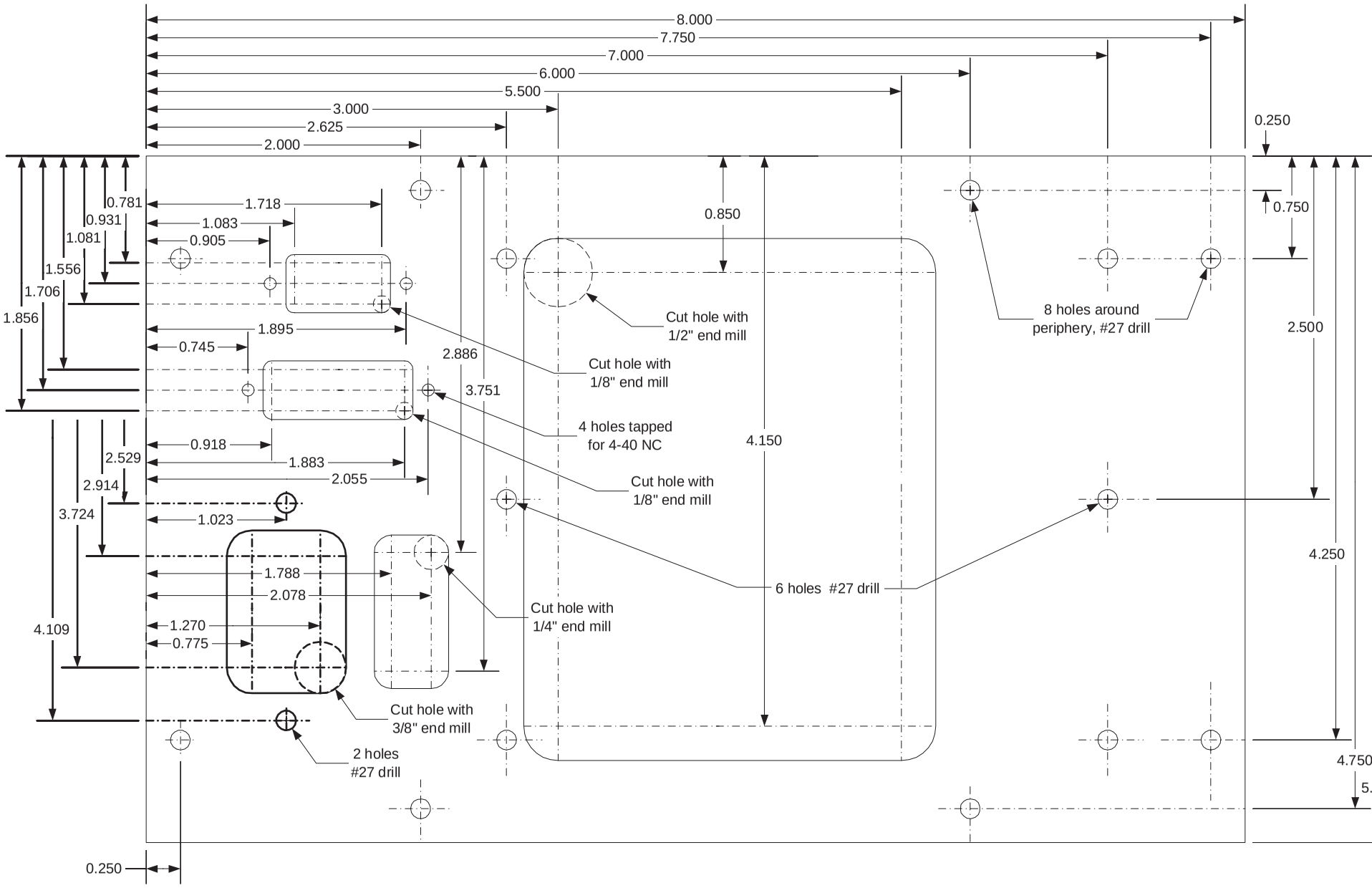

Front Panel: (1 ea) Material: 1/8" 2024 Aluminum sheet.

MSL	TITLE: 3DFM			
	DESCRIPTION: DC prototype drive electronics front panel (rear view)			
DRAWN BY: Leandra Vicci	SIZE: A	DWG NO: Driver 1.3.2		
DATE: 18 April 2001		SCALE: 1: 1	REV: 1	SHEET: 9 OF 13

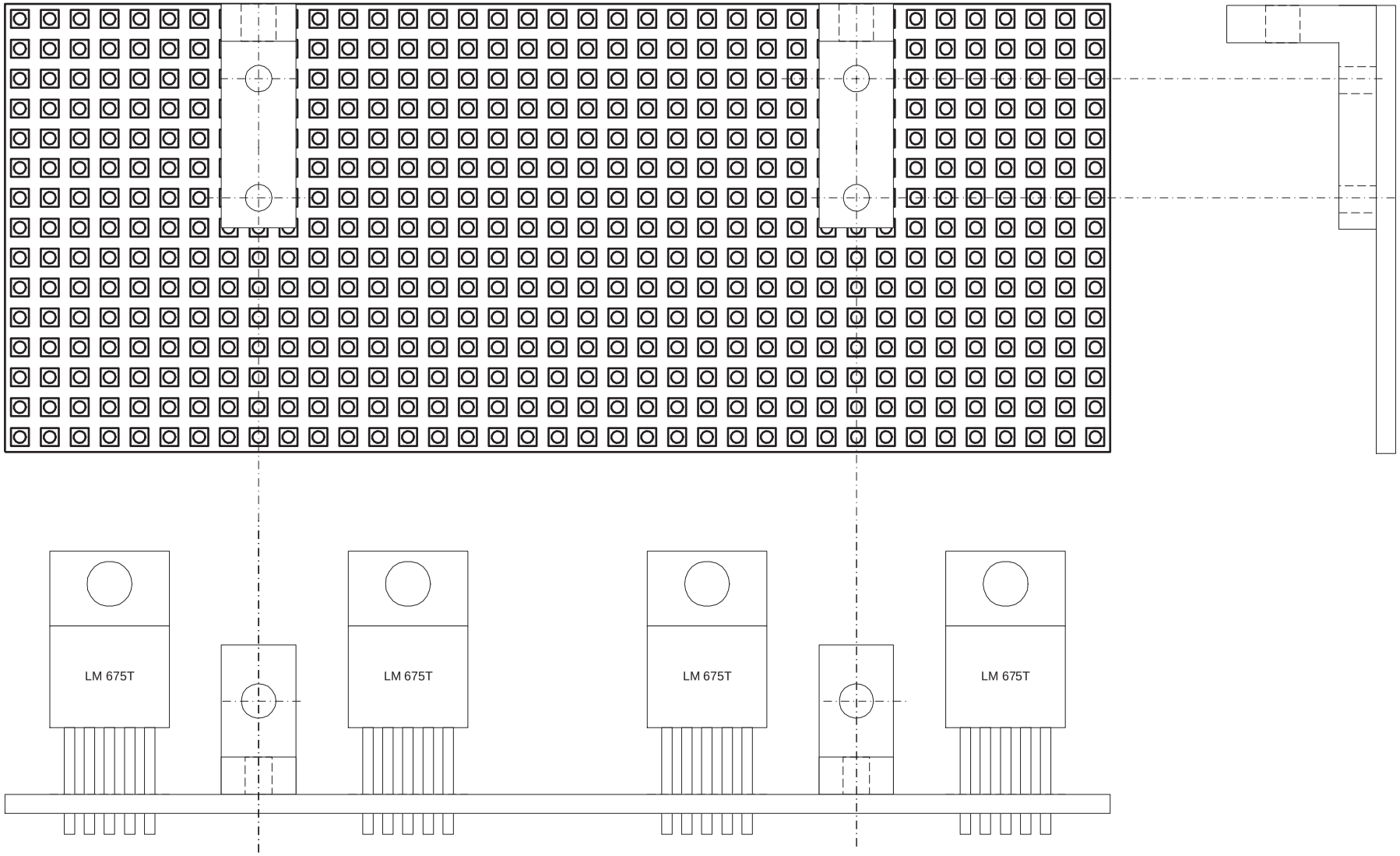

MSL	TITLE: 3DFM				
	DESCRIPTION: DC prototype drive electronics circuit board assembly				
DRAWN BY: Leandra Vicci	SIZE: A	DWG NO: Driver 1.3.3			
DATE: 4 April 2001		SCALE: 2: 1	REV: 0	SHEET: 10 OF 13	

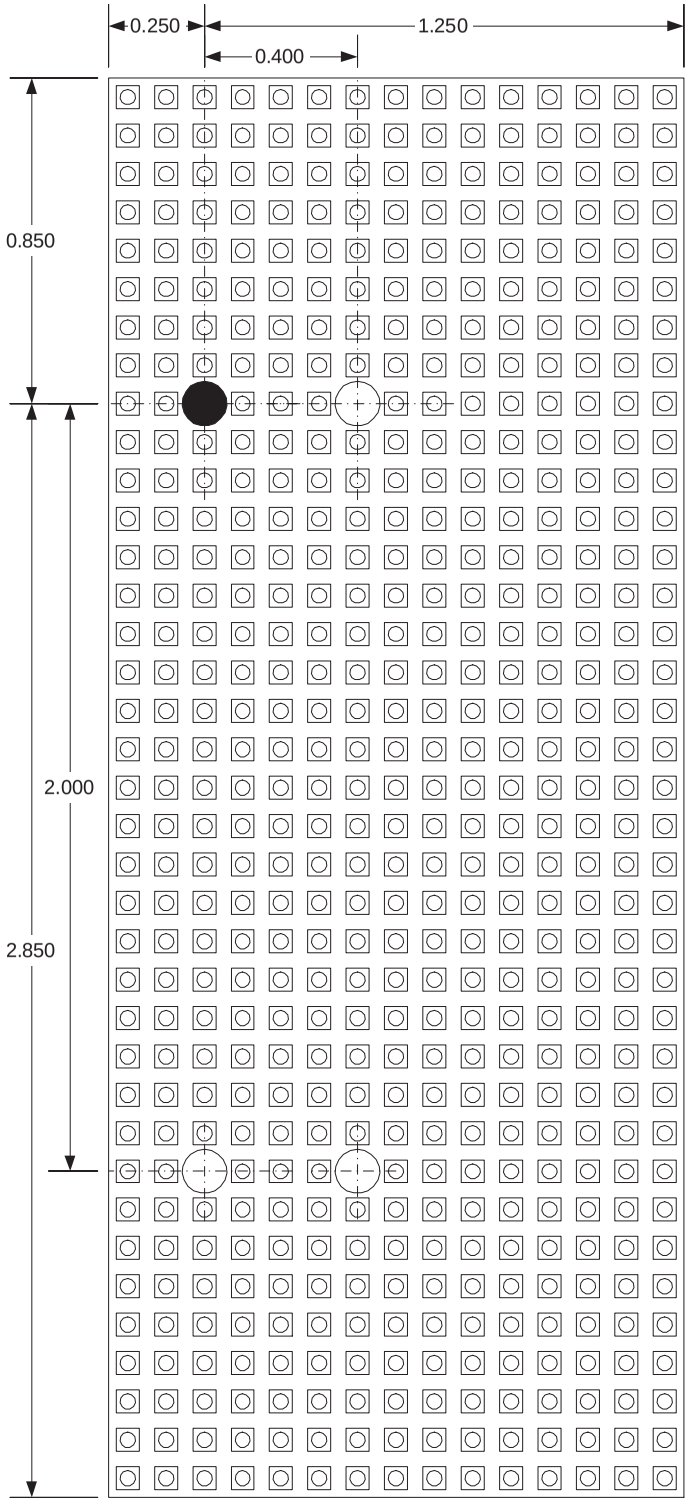

Circuit board (1ea) cut from vectorboard stock 0.060" glass epoxy.
4 holes drilled 0.116" (#32 drill) *centered on existing board holes*.
All board dimensions to be referenced to the hole shown in black.

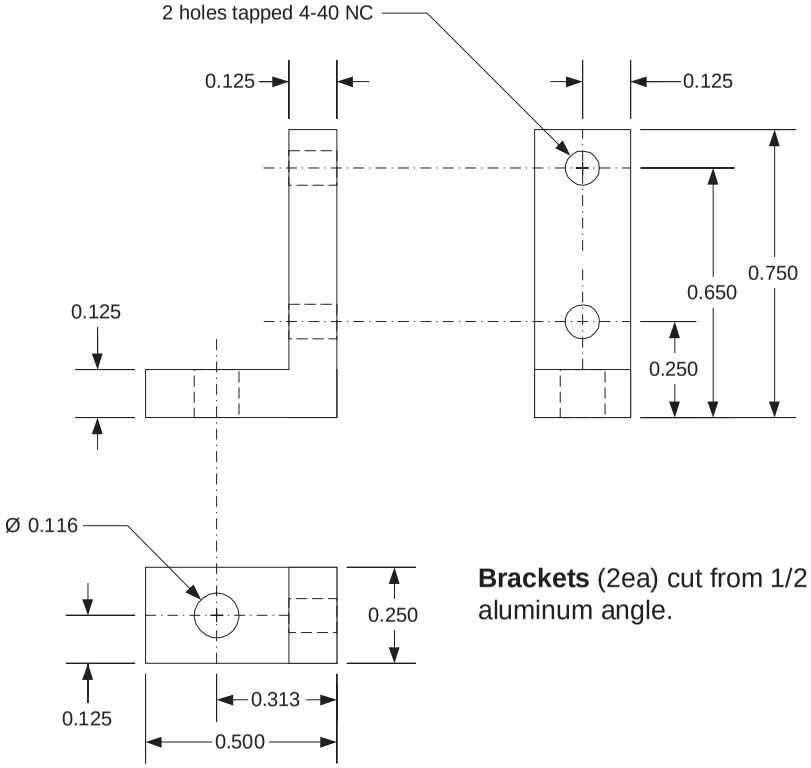

Brackets (2ea) cut from 1/2 x 3/4 x 1/8 aluminum angle.

MSL	TITLE: 3DFM				
	DESCRIPTION: DC prototype drive electronics circuit board and mounting bracket details				
DRAWN BY: Leandra Vicci	SIZE: A	DWG NO: Driver 1.3.4			
DATE: 5 April 2001		SCALE: 2: 1	REV: 0	SHEET: 11 OF 13	

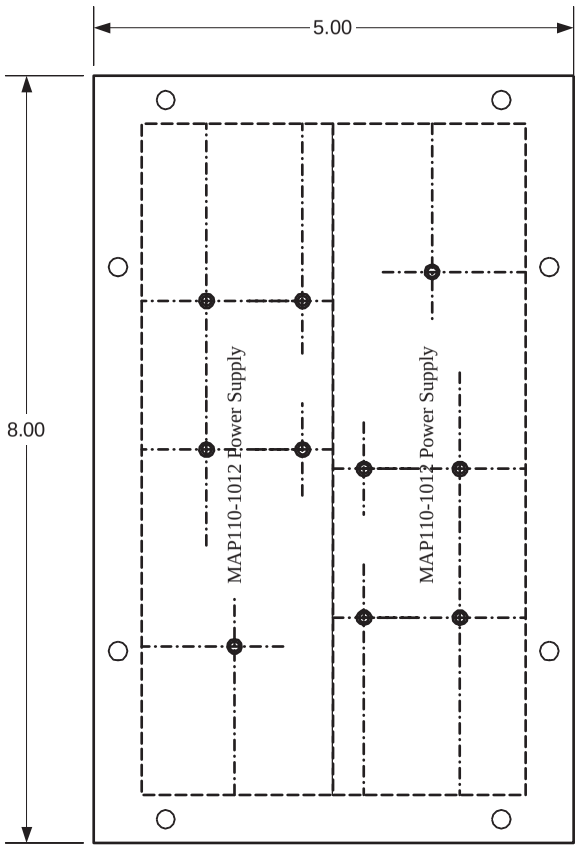

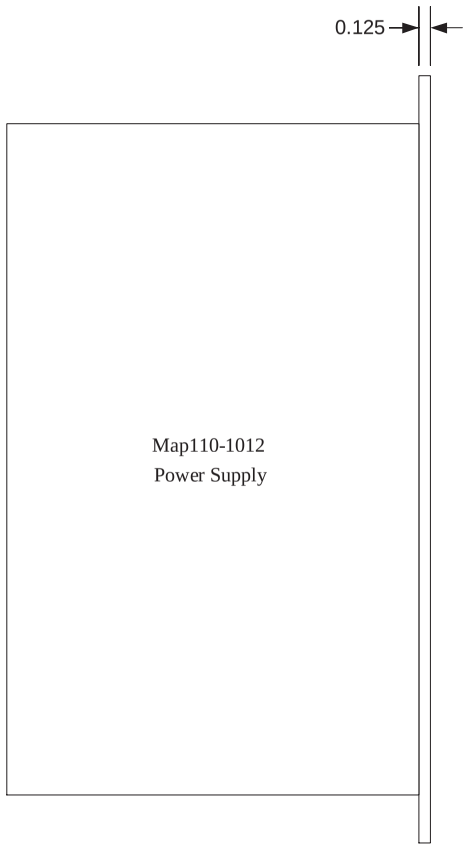

MSL	TITLE: 3DFM					
	DESCRIPTION: DC prototype drive electronics back panel assembly					
DRAWN BY: Leandra Vicci	SIZE: A	DWG NO: Driver 1.4				
DATE: 30 March 2001		SCALE: 1: 2	REV: 0	SHEET: 12 OF 13		

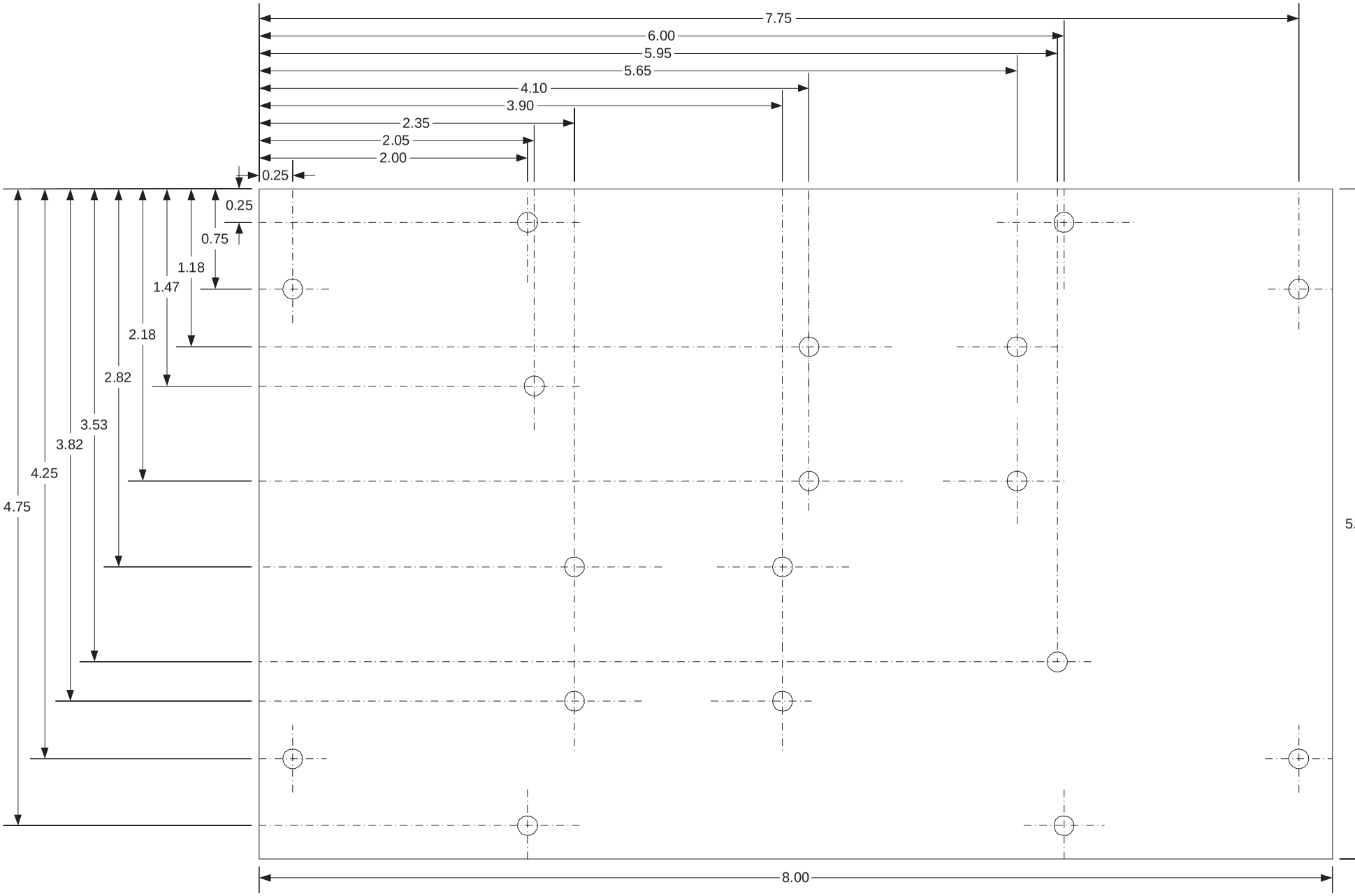

Back Panel: (1 ea) Material: 1/8" 2024 Aluminum sheet.
All holes 0.1495", #25 drill.

MSL	TITLE: 3DFM				
	DESCRIPTION: DC prototype drive electronics back panel				
DRAWN BY: Leandra Vicci	SIZE: A	DWG NO: Driver 1.4.1			
DATE: 18 April 2001		SCALE: 1: 1	REV: 1	SHEET: 13 OF 13	